Vision Research 49 (2009) 2808–2825

Contents lists available at ScienceDirect

Vision Research

journal homepage: www.elsevier.com/locate/visres

Time-course of the retinal nerve fibre layer degeneration after complete intra-orbital optic nerve transection or crush: A comparative study

Guillermo Parrilla-Reverter [a,b,1], Marta Agudo [a,b,1], Francisco Nadal-Nicolás [a], Luis Alarcón-Martínez [a], Manuel Jiménez-López [a], Manuel Salinas-Navarro [a], Paloma Sobrado-Calvo [a], José M. Bernal-Garro [a], María P. Villegas-Pérez [a], Manuel Vidal-Sanz [a,*]

[a] Laboratorio de Oftalmología Experimental, Facultad de Medicina, Universidad de Murcia, 30100 Murcia, Spain
[b] Servicio Murciano de Salud, Hospital Universitario Virgen de la Arrixaca, 30120 Murcia, Spain

ARTICLE INFO

Article history:
Received 10 April 2009
Received in revised form 19 August 2009

Keywords:
Retina
Neurofilament
Optic nerve injury
Neuronal degeneration
Retinal ganglion cell

ABSTRACT

We examined qualitatively and quantitatively in adult rat retinas the temporal degeneration of the nerve fibre layer after intra-orbital optic nerve transection (IONT) or crush (IONC). Retinal ganglion cell (RGC) axons were identified by their heavy neurofilament subunit phosphorylated isoform (pNFH) expression. Optic nerve injury induces a progressive axonal degeneration which after IONT proceeds mainly with abnormal pNFH-accumulations in RCG axons and after IONC in RGCs somas and dendrites. Importantly, this aberrant pNFH-expression pattern starts earlier and is more dramatic after IONT than after IONC, highlighting the importance that the type of injury has on the time-course of RGC degeneration.

1. Introduction

A classic and commonly used model to study the effects of central nervous system neuronal injury is axotomy of the adult mammalian optic nerve (Leoz y Arcuate, 1914; Ramón & Cajal, 1914; Tello, 1907, chap. 5). This model has allowed a number of investigations to study: (i) injury-induced loss of retinal ganglion cells (RGCs) (Lafuente et al., 2002; Lindqvist, Peinado-Ramon, Vidal-Sanz, & Hallbook, 2004; Lindqvist, Vidal-Sanz, & Hallbook, 2002; Marco-Gomariz, Hurtado-Montalban, Vidal-Sanz, Lund, & Villegas-Pérez, 2006; Nadal-Nicolás et al., 2009; Parrilla-Reverter et al., 2009; Villegas-Pérez, Lawrence, Vidal-Sanz, Lavail, & Lund, 1998; Villegas-Pérez, Vidal-Sanz, & Lund, 1996; Villegas-Pérez, Vidal-Sanz, Rasminsky, Bray, & Aguayo, 1993; Wang et al., 2003; Wang, Villegas-Pérez, Vidal-Sanz, & Lund, 2000); (ii) the prevention of such a loss using neuroprotective substances (Aviles-Trigueros et al., 2003, Lafuente Lopez-Herrera, Mayor-Torroglosa, Miralles d, Villegas-Pérez, & Vidal-Sanz, 2002; Lafuente et al., 2002; Mayor-Torroglosa et al., 2005; Parrilla-Reverter et al., 2009; Peinado-Ramon, Salvador, Villegas-Pérez, & Vidal-Sanz, 1996; Vidal-Sanz, Aviles-Trigueros, Whiteley, Sauve, & Lund, 2002; Vidal-Sanz et al., 2007; Vidal-Sanz, Lafuente, Mayor, de Imperial, & Villegas-Pérez, 2001), (iii) the molecular and functional changes associated to RGC injury (Agudo et al., 2008; Agudo et al., 2009; Chidlow, Casson, Sobrado-Calvo, Vidal-Sanz, & Osborne, 2005; Nadal-Nicolás et al. 2009, Salvador-Silva, Vidal-Sanz, & Villegas-Pérez, 2000; Sobrado-Calvo, Vidal-Sanz, & Villegas-Pérez, 2007) and; (iv) the capacity of these injured neurons to regenerate their axons, reinnervate their targets and form synapses (Aviles-Trigueros, Sauve, Lund, & Vidal-Sanz, 2000; Bahr, Eschweiler, & Wolburg, 1992; Cho & So, 1989; Robinson, 1994; Sasaki et al., 1996; Thanos & Vanselow, 1989; Vidal-Sanz, Bray, & Aguayo, 1991; Vidal-Sanz, Bray, Villegas-Pérez, Thanos, & Aguayo, 1987; Vidal-Sanz et al., 2002; Watanabe, Sawai, & Fukuda, 1991; Whiteley, Sauve, Aviles-Trigueros, Vidal-Sanz, & Lund, 1998).

These studies have shown that injury to retinal ganglion cell axons [i.e. to the optic nerve (ON)] induces the death of the parent neurons, the RGCs (Villegas-Pérez, Vidal-Sanz, Bray, & Aguayo, 1988; Villegas-Pérez et al., 1993), and that the severity of this loss depends on a number of variables, such as the quantity of axons affected by the lesion, which may vary from a partial compression of the ON (Yoles & Schwartz, 1998) to a complete crush or transection (Burke, Cottee, Garvey, Kumarasinghe, & Kyriacou, 1986; Villegas-Pérez et al., 1988), the distance from the cell soma where the lesion is performed, as the longer the distance from the cell soma

Abbreviations: IONC, intra-orbital optic nerve crush; IONT, intra-orbital optic nerve transection; RGCs, retinal ganglion cells; pNFH, phosporylated isoform of the heavy neurofilament subunit.

* Corresponding author. Fax: +34 968 363962.
E-mail address: ofmmv01@um.es (M. Vidal-Sanz).

[1] These authors contributed equally towards this work.

0042-6989/$ - see front matter © 2009 Elsevier Ltd. All rights reserved.
doi:10.1016/j.visres.2009.08.020

at which the lesion is inflicted, the slower the rate of RGC loss is (Berkelaar, Clarke, Wang, Bray, & Aguayo, 1994; Villegas-Pérez et al., 1993), and the type of injury (for review see Parrilla-Reverter et al., 2009), because axotomy-induced RGC degeneration is quicker and more severe after optic nerve transection (Mansour-Robbaey et al., 1994; Nadal-Nicolás et al., 2009; Peinado-Ramon et al., 1996; Villegas-Pérez et al., 1993) than after optic nerve crush (Berkelaar et al., 1994; Nadal-Nicolás et al., 2009; Parrilla-Reverter et al., 2009). The relative importance of the type of injury caused upon the retinofugal pathway has been underscored by a recent study in which the retinal transcriptome profile from IONC and IONT retinas was examined and compared to naïve retinas using affymetrix RAE230.2 arrays (Agudo et al., 2008), and by a detailed analysis of the pattern and temporal course of RGC loss induced by such injuries (Nadal-Nicolás et al., 2009; Parrilla-Reverter et al., 2009; Peinado-Ramon et al., 1996). In the present studies we have further investigated the effects that the type of injury; whether axotomy is performed by ON transection or crush, have on the degenerative events that take place in the nerve fibre layer of the retina.

Axonal degeneration after optic nerve injury is a progressive alteration that was described by Ramón y Cajal (1914, chap. 5) and his collaborators (Leoz y Arcuate, 1914; Tello, 1907) using the neurofibrilar silver nitrate staining. Neurofilaments (NF) represent the main cytoskeletal proteins in mature neurons and are responsible for maintaining the calibre of myelinated axons and consequently their conduction velocity. NFs are assembled from three subunits, classified according to their molecular weight into high (H), medium (M) and low (L). These proteins are modified by post-translational changes, wherein the most significant is phosphorylation that regulates their assembly and interactions. Phosphorylation of NF, in particular NFH, has long been considered to decrease their transport rate (for review see Perrot, Berges, Bocquet, & Eyer, 2008). In fact, highly phosphorylated isoforms of NFH (pNFH) are present only in mature axons whilst dephosphorylated isoforms are found in the neuronal soma and dendrites (Perrot et al., 2008; Sternberger, Sternberger, & Ulrich, 1985). Abnormal organisation and/or metabolism of NF are associated with several human neurodegenerative diseases and experimentally damaged neurons (Buckingham et al., 2008; Dieterich et al., 2002; Soto et al., 2008, for review see Al Chalabi & Miller, 2003; Perrot et al., 2008; Petzold, 2005; Salinas-Navarro et al., submitted for publication). In these paradigms highly phosphorylated NFH are often accumulated in the neuronal body. After different types of retinal injuries such as ischemia, excitotoxicity and optic nerve axotomy there is a decrease in the mRNA levels of NFs (Agudo et al., 2008; Chidlow et al., 2005; Hoffman, Pollock, & Striph, 1993; McKerracher, Vidal-Sanz, Essagian, & Aguayo, 1990) which, in the case of ON injury, correlates with an impairment of their axonal transport if the RGCs are committed to death (McKerracher, Vidal-Sanz, & Aguayo, 1990) but not if RGCs are allowed to regenerate along segments of peripheral nerve grafted to the ocular stump of the intraorbitally transected optic nerve (McKerracher, Vidal-Sanz, Aguayo, 1990; Vidal-Sanz, Villegas-Pérez, Bray, & Aguayo, 1993; Vidal-Sanz et al., 2002).

Axons were identified by immunodetection of pNHF using the RT97 monoclonal antibody. This antibody recognizes the phosphorylated isoform of the heavy subunit of neurofilaments (Drager & Hofbauer, 1984; Veeranna et al., 2008) which, in healthy neurons, is expressed in mature axons. In fact, the medium and heavy neurofilament subunits are poorly or not at all phosphorylated in the somato-dendritic neuronal compartment whereas they are highly phosphorylated in the axonal one (Gotow, Tanaka, & Takeda, 1995; Lewis & Nixon, 1988; Petzold, 2005). Furthermore, it has been shown that after axonal damage, certain cells have an abnormal pNFH distribution in their soma and dendrites (Drager & Hofbauer, 1984) and this aberrant distribution has been demonstrated as well in a variety of human and experimental neuronal disorders (for review see Al Chalabi & Miller, 2003; Perrot et al., 2008; Petzold, 2005), including RGC axonal injury (Marco-Gomariz et al., 2006; Salinas-Navarro et al., submitted for publication; Vidal-Sanz et al., 1987; Villegas-Pérez et al., 1988; Villegas-Pérez et al., 1996; Villegas-Pérez et al., 1998; Wang et al., 2000; Wang et al., 2003).

In the present studies using the RT97 antibody, we have analyzed qualitative and quantitatively, the abnormal expression of pNFH, in particular their distribution within the RGCs axons, somas and processes, as well as its time-course and topological distribution within the retina. Although similar events were found in both situations, there were some differences in the pattern and course of axonal degeneration among both injuries. In general, the number of RGCs with abnormal expression of pNFH ($RT97^+$RGCs) was greater after IONC than after IONT. Their distribution throughout the retina tended to be random, although they first appeared within the periphery and middle retina evolving to include the central retina. Overall, the present results about the aberrant expression of pNFH, plus our recent studies about the time-course of RGC loss induced by axotomy, (Nadal-Nicolás et al., 2009; Parrilla-Reverter et al., 2009) together with the different gene regulation response induced by these injuries (Agudo et al., 2008; Agudo et al., 2009) highlight the importance that the type of injury inflicted to the ON has on severity and the speed of axotomy–induced RGC loss and on the molecular events leading to their degeneration [Short accounts of this work were presented in abstract form (Parrilla-Reverter et al., 2006)].

2. Materials and methods

2.1. Animal handling

Adult female Sprague–Dawley rats (180–220 g body weight) were obtained from the University of Murcia breeding colony. For anaesthesia a mixture of xylazine (10 mg/kg body weight; Rompun®; Bayer, Kiel, Germany) and ketamine (60 mg/kg body weight; Ketolar®; Pfizer, Alcobendas, Madrid, Spain) was used intraperitoneally (i.p.). All experimental procedures were carried out in accordance with our institutional rules, European Union regulations and the Association for Research in Vision and Ophthalmology guidelines for the use of animals in research. Right after the surgical manipulation and during recovery from anaesthesia an ointment containing neomycin and prednisone (Oftalmolosa Cusí Prednisona-Neomicina®; Alcon S.A., Barcelona, Sapin) was applied on the cornea to prevent corneal desiccation. Additional measures were taken to minimize pain or discomfort. Animals were sacrificed with an i.p. injection of an overdose of pentobarbital (Dolethal Vetoquinol®; Especialidades Veterinarias, S.A., Alcobendas, Madrid, Spain).

2.2. Optic nerve injury

The left optic nerve (ON) was injured intraorbitally according to procedures that are commonly used in our laboratory (Lafuente Lopez-Herrera et al., 2002, for review see Vidal-Sanz et al., 1993). In the group of rats undergoing intra-orbital optic nerve transection (IONT), the ON was severed at approximately 3 mm from the optic disk. To access the ON at the back of the eye, an incision was made in the skin overlying the superior orbital rim, the supero-external orbital contents were dissected, and the superior and external rectus muscles were sectioned. The duramater of the ON was opened longitudinally, and the ON was completely transected. Care was taken not to damage the retinal blood supply, which enters the eye separately in the inferonasal aspect of the ON sheath (Morrison, Johnson, Cepurna, & Funk, 1999). In the group of rats undergoing intra-orbital optic nerve crush (IONC) the ON was accessed as before

but without opening the duramater, then it was completely crushed during 10 s at 3 mm from the optic disk using watchmaker's forceps as recently described (Parrilla-Reverter et al., 2009). We did not control the pressure applied in this study. However, the validation of the methodology employed to induce complete optic nerve crush was previously reported in our parallel study (Parrilla-Reverter et al., 2009), in which several control experiments using orthograde as well as retrograde tracers demonstrated that our crush injury methodology involved axotomy of the entire population of RGCs. Finally, before and after either of the surgical procedures, the eye fundus was observed through the operating microscope to assess the integrity of the retinal blood flow.

For our qualitative study, animals undergoing IONC or IONT were sacrificed at 3, 7, 10, 12, 15, 21, 30 or 90 ($n = 8$ retinas per group and time-point except at 3 days that was $n = 4$) days post-injury. In addition to the right (contralateral) retinas of the injured animals, four naïve retinas from intact animals were used as controls.

For our quantitative study, the number of analyzed retinas were: naïve ($n = 4$); right eyes ($n = 8$); IONT: 3 d ($n = 4$), 7 d ($n = 8$); 14 d ($n = 8$), 21 d ($n = 5$); 30 d ($n = 5$); IONC: 3 d ($n = 4$), 7 d ($n = 4$), 14 d ($n = 8$), 21 d ($n = 6$), 30 d ($n = 8$).

2.3. Identification of rgcs: retrograde tracing with dtmr or fluorogold

To study whether the RT97 immunofluorescence cells that appeared after ON injury were RGCs and not other retinal neurons, two additional groups were prepared following previously described methods (Lafuente, Villegas-Pérez, Mayor, et al., 2002; Lafuente, Villegas-Pérez, Selles-Navarro, 2002; Salinas-Navarro, Mayor-Torroglosa, et al., 2009). The passively transported retrograde tracer dextran tetramethylrhodamine (DTMR; 3000 MW; Molecular Probes, Inc., Eugene, OR, USA) was applied to the optic nerve stump in six rats processed 30 days after IONC and 2 days prior to sacrifice. The actively transported retrograde tracer, fluorogold (FG, 3% diluted in 10% DMSO-saline, Fluorochrome, LLC, USA) was applied to the optic nerve stump of seven rats 14 days after IONC and 3 days prior to sacrifice. In brief, small crystals of DMTR or small pieces of gel-foam soaked in FG; were applied to the ocular stump of the left ON, which had been intraorbitally re-transected, this time at approximately 0.5 mm from the eye. Both tracers diffuse through the axon towards the cell soma producing an intense labelling (Salinas-Navarro et al., 2009; WoldeMussie, Ruiz, Wijono, & Wheeler, 2001). These tracers would identify those RGCs that survive the lesion.

2.4. Immunohistofluorescence analysis

All animals were deeply anaesthetized with an overdose of sodium penthobarbital and perfused transcardially with 4% paraformaldehyde in 0.1 M phosphate buffer after a saline rinse. Retinas from both eyes were dissected as flattened whole-mounts as previously reported (Nadal-Nicolás et al., 2009; Salinas-Navarro et al., 2009; Salinas-Navarro, Mayor-Torroglosa, et al., 2009; Wang et al., 2000; Wang et al., 2003). All retinas were immunostained using the monoclonal antibody RT97. The RT97 antibody developed by John Wood (Wood & Anderton, 1981) was obtained from the Developmental Studies Hybridoma Bank developed under the auspices of the NICHD and maintained by the University of Iowa, Department of Biological Sciences, Iowa City, IA 52242). RT97 is a monoclonal IgG1, raised in mouse against Wistar rat neurofilaments, that recognizes, in Western blots, the phosphorylated isoforms of the 200 and 145 kDa neurofilament subunits (Anderton et al., 1982; Veeranna et al., 2008; Wood & Anderton, 1981), and also phosphorylated epitopes of Tau and MAP 1B (Anderton et al., 1982; Cairns et al., 1997; Coleman & Anderton, 1990; Johnstone, Goold, Fischer, & Gordon-Weeks, 1997; Ksiezak-Reding, Dickson, Davies, & Yen, 1987; for review see Marco-Gomariz et al., 2006). This antibody in the mammalian retina labels retinal ganglion cell axons, photoreceptor outer segments, and horizontal cells (Balkema & Drager, 1985; Drager & Hofbauer, 1984). We have a long experience with the commercial RT97 antibody which, in our hands, labels intensely RGC axons and some injured RGC bodies and occasionally faintly the horizontal cell plexus (Marco-Gomariz et al., 2006; Salinas-Navarro et al., submitted for publication; Vidal-Sanz et al., 1987; Villegas-Pérez et al., 1988; Villegas-Pérez et al., 1996; Villegas-Pérez et al., 1998).

Immunodetection was done using protocols that are standard in our laboratory (Marco-Gomariz et al., 2006; Villegas-Pérez et al., 1988, 1996, 1998; Wang et al., 2000, 2003). In brief: retinas were incubated 1 h at room temperature (RT) in blocking buffer (Triton 2% and 2.5% bovine serum albumin in phosphate buffered saline-PBS) followed by overnight incubation at 4 °C with the primary antibody diluted 1:1000 in the same blocking buffer. The following day retinas were washed in PBS (3×10 min at RT) and secondary detection was carried out by 1 h incubation at room temperature with goat anti-mouse-FITC antibody (F-4018, Sigma–Aldrich, St. Louis, Missouri, USA) diluted 1:50 in blocking buffer. After that, retinas were washed in PBS, mounted vitreal side up on gelatin-coated slides, with antifading mounting media containing 50% glycerol and 0.04% p-phenylenediamine in 0.1 M sodium carbonate buffer (pH 9).

2.5. Retinal imaging and analysis

All whole-mounted retinas (left and right eyes) were analyzed for RT97 signal. DTMR or FG signal were also acquired in those retinas labelled with either tracer. Individual and magnified images were taken with an epifluorescence microscope (Axioscop 2 Plus; Zeiss Mikroskopie, Jena, Germany) using the Image Pro Plus software, (IPP 5.1 for Windows®; Media Cybernetics, Silver Spring, MD, USA), as previously described (Marco-Gomariz et al., 2006; Nadal-Nicolás et al., 2009; Salinas-Navarro, Mayor-Torroglosa, et al., 2009). Briefly: to make reconstructions of retinal whole-mounts, retinal multiframe acquisitions were photographed in a raster scan pattern where the frames were captured contiguously side-by-side with no gap or overlap between them using an 10× objective (Plan-Neofluar, 10×/0.30; Zeiss Mikroskopie, Jena, Germany). Single frames were focused manually prior to the capture of the digitized images which were then fed into the image analysis program. The plane of focusing was between the RGC and the nerve fibre layer of the retina. Depending of the retina size and orientation on the slide a scan area is defined to cover completely the whole retina. This scan area consists of a matrix of m frames in columns and n frames in rows, where the total number of frames in the scan area is indicated by frames in columns times frames in rows ($m \times n$). The frame size is 840×623 pixels and usually, 140 images had to be taken for each retina. The capture calibration is 1 pixel equals to 0.0011 mm. All images were captured at a resolution of 300 dpi.

The images taken for each retina were saved in a folder as a set of 24-bit color image pictures. Later, these images can be combined automatically into a single tiled high resolution composite image of the whole retina using IPP® for Windows®. Reconstructed images were further processed with an image-editing computer software (Adobe Photoshop® CS; ver 8.0.1, Adobe Systems, Inc., San Jose, CA) when correct orientation of the retina was needed.

2.6. Quantitative retinal analysis

2.6.1. pNFH fluorescence area

Whole-mount images from each retina were processed by a specific subroutine developed to automate repetitive tasks. In brief,

the IPP macro language was used to apply a sequence of filters and transformations in order to obtain the fluorescent area as well as the total area of the central, medial, and peripheral parts of the retina. In a first step, the contour of the retina was outlined on the whole-mount image, creating a new area of interest, the flatten filter was applied just on that area of interest, reducing the variations on background intensity, the total area of the retina (mm^2) was also obtained and saved into an excel sheet (Microsoft® Office Excel 2003, Microsoft Corporation, Redmond, WA, USA). The next step was to situate five points on the retina, the first one on the optic nerve disk, and the other four on the edge of each retinal quadrant, in order to calculate the minimum distance between the optic nerve and those points. The optic nerve area was deleted and the minimum distance was used to create three equidistant rings, one for each retinal area: central, medial, and peripheral (see Fig. 9D). For each ring two processes were launched: one to calculate the area occupied by fluorescence and the other to calculate its total area (both in mm^2). To calculate the fluorescent area, the image of each retinal ring (central, medial or peripheral) was converted into a grey scale, and the user carried out an histogram segmentation selecting all the objects that were fluorescent, the area of that selection was exported to the same excel sheet. To calculate the total area of each ring, the user performed an histogram segmentation on the original ring image to select and obtain its whole area, which was exported to the excel sheet. The percentage of each ring occupied by RT97 fluorescence was calculated using the fluorescent area in each ring referred to its whole area which was arbitrarily considered 100%.

2.6.2. pNFH-positive RGCs localization and spatial distribution in the retina

The numbers of RGCs expressing aberrant RT97 staining of their soma were counted in a masked fashion in experimental as well as in control retinas. At first the retinal whole-mount images were edited using Adobe Photoshop, the whole retina was examined at high magnification frame by frame, and every $RT97^+$RGC was marked with a dot of different color to distinguish faint or intense RT97 immunofluorescence (Fig. 8C shows an example of both intensities). For the two types of cells, a counting routine developed into Image Pro Plus macro language was launched: the user is first asked to point the optic nerve disk, in order to perform a translation of that point to the origin of the cartesian coordinate system; then the counting routine obtained the total number of blue or red dots in the image, evaluated their spatial position, and translated it in relation to the origin. The information (number of dots and their coordinates) was exported into an excel sheet.

The spatial distribution of FG^+RGCs in every analyzed retina was evident from the whole-mount images edited with Adobe Photoshop and marked with dots to indicate the location of these neurons. To illustrate this matter more graphically, we chose three representative retinas from each experimental group and timepoint and their $RT97^+$RGCs were pooled into a single diagram constructed with the aid of SigmaPlot 9 software (SigmaPlot® 9.0 for Windows®, Systat Software, Inc., Richmond, CA) (See below, Fig. 7).

2.6.3. Quantification of RT97 positive neurons that were also retrogradely labelled with Fluorogold

Our quantitative analysis (see below) indicated that abnormal RT97 immunofluorescence within injured RGCs peaked around 14 days, thus we examined in a masked fashion a group of rats in which FG was applied to the ON head stump three days prior to sacrifice and 14 days after IONC. In these retinas ($n = 7$), randomly selected images ($n = 8$ per retina) spanning the entire retina were obtained under the UV (for FG fluorescence) and the FITC (for RT97 immunofluorescence) filter. FG and RT97 images were coupled using the Adobe Photoshop program and the numbers of $RT97^+$RGCs as well as those that were also positive for FG were counted.

2.6.4. Statistical analysis

Data is shown as mean ± SEM. Statistical analysis of the differences between groups of retinas or groups of animals was done using non-parametric ANOVA tests using Sigma Stats® 3.5 for Windows® (Systat Software, Inc., Richmond, CA) software. Differences were considered significant when $p < 0.05$.

3. Results

In the present work we have studied qualitative and quantitatively, in whole-mounted retinas the time-course of axotomy-induced RGC axonal degeneration and compared the effects that IONT and IONC have on it. Our data show that optic nerve injury results in abnormal expression of pNFH within axons, cell bodies and primary dendrites of RGCs. Abnormal signal of RT97 immunoreactivity appears as early as 3 days post-injury near the cell body and spreads somatofugally along the nerve fibres. Abnormal pNFH-expression patterns range from intra-axonal deposits shaped like rosary-beads and small varicosities to accumulations within the RGCs bodies, the former being more frequently found in IONT-injured retinas and the latter in IONC-injured ones. Axonal loss appears in the centre of the retina earlier after IONT than IONC, interestingly, after both lesions $pNFH^+$ axons reach the medial and peripheral retina, an abnormal expression pattern that is not found in control retinas. $pNFH^+$RGCs first appear mainly in the peripheral and middle retina spreading towards the central retina, peaking at 14 days after axotomy and there were greater numbers in IONC than in IONT retinas. We also provide additional evidence documenting that abnormal expression of pNFH only occurs in injured retinal ganglion cells and not in other retinal neurons. Finally, this works demonstrates that these changes in pNFH-expression pattern are early events of axotomy-induced RGC degeneration that last, at least, up to 90 days post-injury.

3.1. Qualitative analysis

3.1.1. Neurofilament staining in control retinas

RGC axons were detected by their RT97 immunoreactivity and thus by their expression of the phosphorylated isoform of the neurofilament heavy subunit (pNFH). A representative photomontage of a control retina (Fig. 1A) shows the typical RT97 immunoreactivity present in bundles of RGC axons. The signal is usually intense at the centre of the retina, where RGC axons running from the periphery towards the centre, converge radially into tightly packed bundles (Fig. 1B–D) to form the optic disk (Fig. 1B). These axons are uniformly labelled and their morphology is rectilinear. It is worth noting that in control retinas (naïve or contralateral to injured retinas) pNFH-signal did not reach the periphery of the retina (Fig. 1A and E) nor was observed in the cell bodies or dendrites of RGCs.

3.1.2. Neurofilament staining after IONT or IONC

The pattern of pNFH-expression in retinas whose ON had been injured with either IONT or IONC was analyzed at 3, 7, 10, 12, 14, 21, 30 or 90 days after injury. In general, there were abnormal distributions of pNFH within the intraretinal aspect of the axon as well as within the cell bodies and dendrites of some RGCs.

At three and seven days post-IONT or IONC there were no noticeably changes on pNFH-expression when the retinas were examined at low magnification (Fig. 2C and D); indeed RT97 signal in the central retina of these damaged retinas does not differ from that observed in control ones. Higher magnification examination *three days* post-IONT and IONC, showed aberrant pNFH-signal was al-

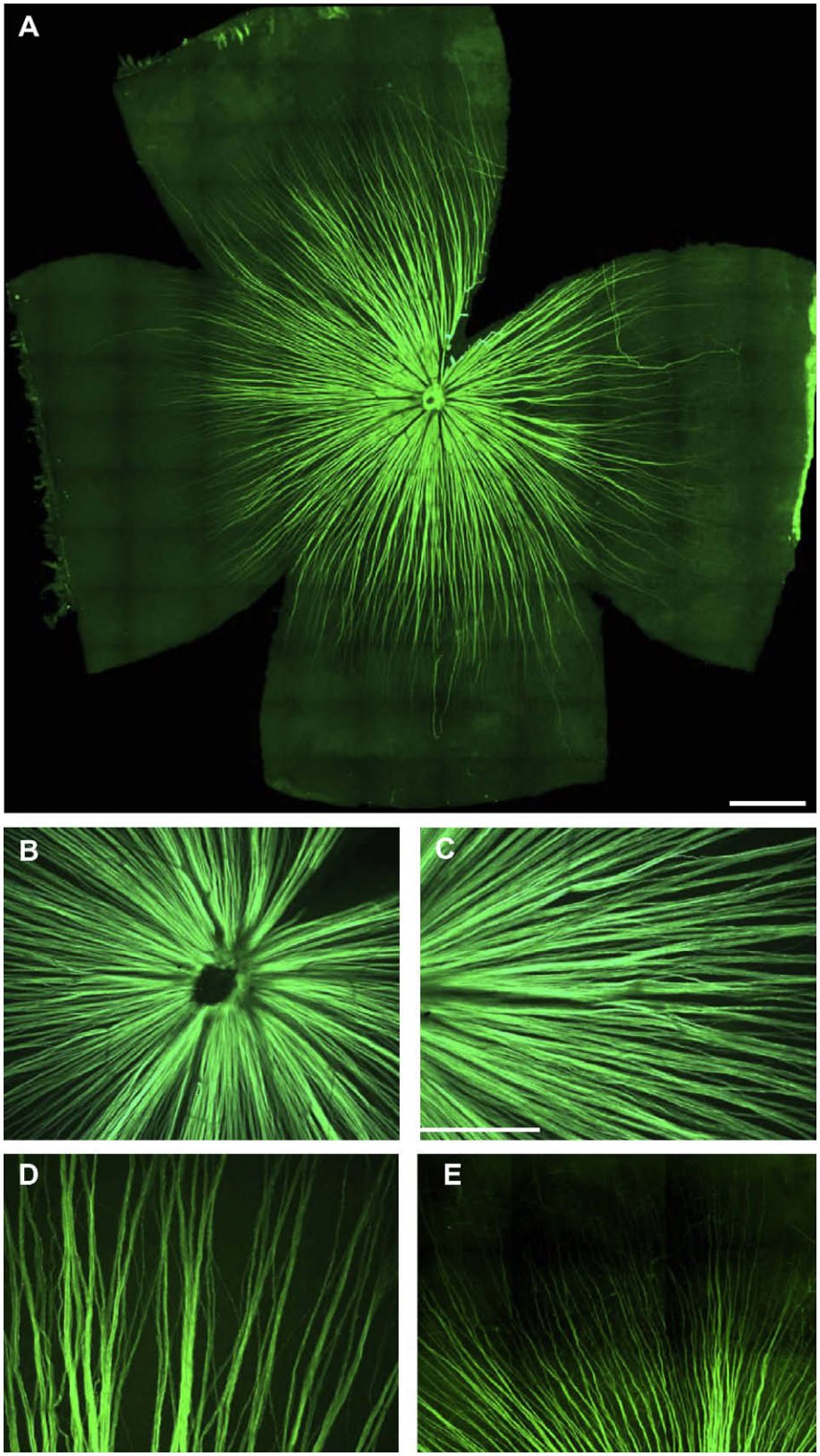

Fig. 1. Expression pattern of RT97 immunoreactivity in control retinas. (A) Whole-mounted retina immunostained for pNFH. (B) pNFH-expression pattern in the central area of a control retina, notice all immunostained RGC axons radially converging towards the optic disk. (C and D) pNFH-expression pattern in the middle region of a control retina. (E) pNFH-expression pattern at the periphery of a control retina. Note that few axons are pNFH-positive. *Abbreviations:* pNFH: phosphorylated neurofilament heavy subunit, Bars: A: 1 mm, B–E: 200 μm. Right: temporal, top: superior except in A and B where the superior pole is situated at 1 o'clock.

ready observed at the peripheral retina (Fig. 2A and B) and in addition faintly stained RGCs appear mainly within the peripheral and middle retina (see below). At *seven days* post-injury, inspection of the retinal periphery disclosed that after IONT, some RGC axons

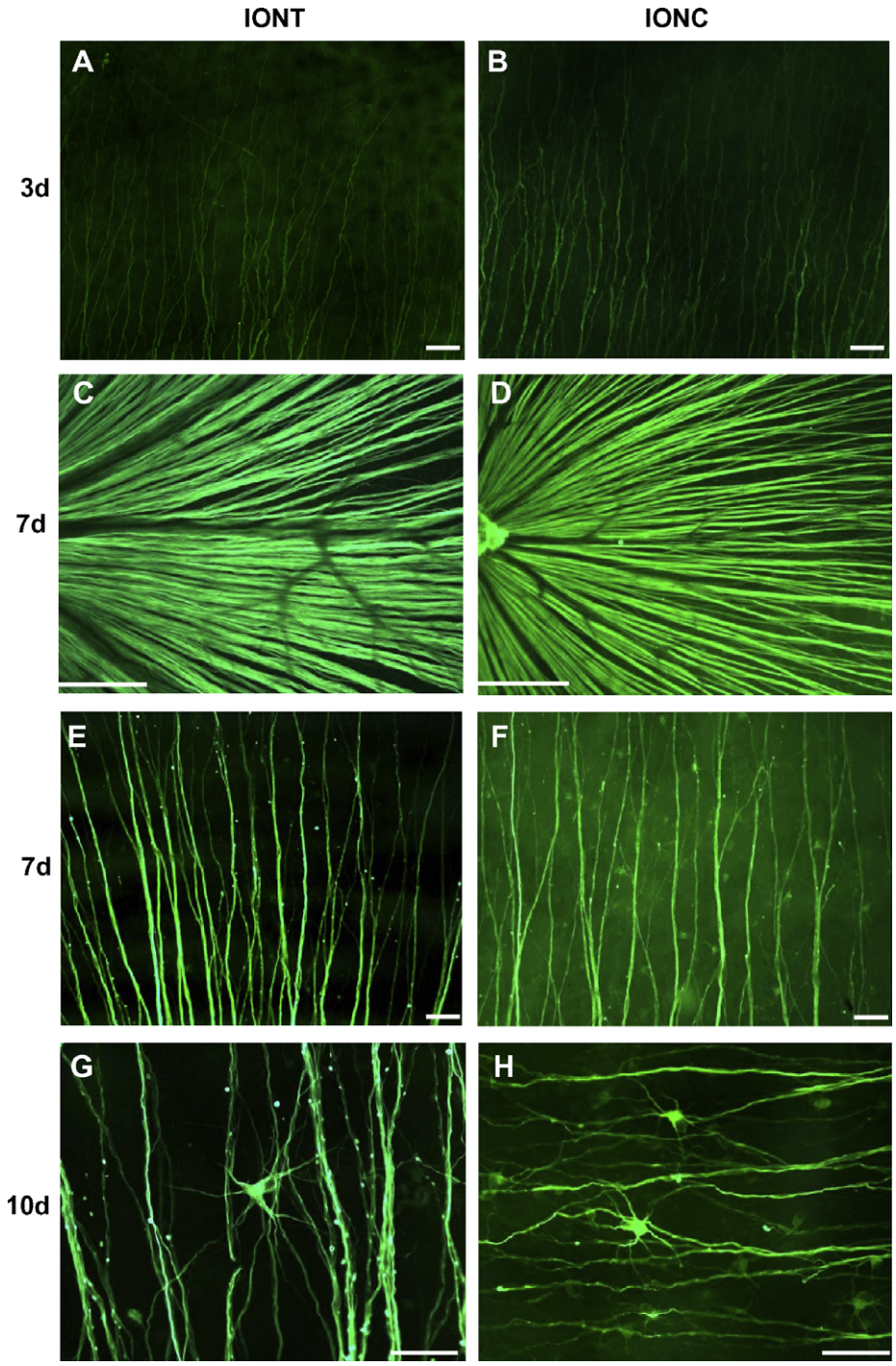

Fig. 2. Changes of the expression pattern of RT97 immunoreactivity 3, 7 or 10 days after IONT or IONC. Three days after IONT (A) or IONC (B) RT97 aberrant signal in the peripheral retina is already observed. The pNFH-expression pattern in the centre of the retina seven days after IONT (C) or IONC (D) does not differ from control retinas. However pNFH-aberrant accumulations are observed in the peripheral areas. At this time-point there are already some differences between both injuries with many axonal accumulations of pNFH after IONT (E) whereas many cell bodies exhibit pNFH-signal after IONC (F). Ten days after IONT, intra-axonal pNFH-accumulations are more evident, and some cell bodies start to show RT97 immunoreactivity (G). However after IONC (H) there are few pNFH-accumulations but a higher number of pNFH-positive cell bodies are observed. Top: superior, right: temporal. *Abbreviations:* IONT: intra-orbital nerve transection, IONC: intra-orbital nerve crush, d: days post-lesion. pNFH: phosphorylated neurofilament heavy subunit. Bars: A, C: 200 μm, B, D, E, F: 50 μm.

showed a varicose morphology with bead-like structures highly positive for RT97 on the portion of the axon located at the retinal periphery (Fig. 2E). Moreover, some RGC bodies and their proximal dendrites also appeared stained with RT97 and occasionally it was possible to appreciate simultaneously RT97 labelling in the cell soma, its primary dendrites and its axon. After IONC, a thorough analysis of the periphery also showed some abnormalities in axonal morphology and the aberrant pNFH-expression in cell bodies was more abundant than after IONT (Fig. 2F). The degree of RT97 labelling within the cell soma and their primary dendrites varied from a faint but clear staining to a very intense labelling throughout the soma and dendrites. All these changes progressed with time and were more evident by *10 days* post-injury (Fig. 2G and H).

At day 12 post-IONT the centre of the retina shows signs of axonal degeneration; there are fewer axons present (Fig. 3A) and varicosities appear in these axons all throughout their extension, from

the retinal periphery to the optic disk (Fig. 3B). The peripheral retina shows intense RT97 stained axons that instead of arising from normal looking RGC bodies, emerge from a cell soma RT97 immunopositive with a club- flare- or bulb-like morphology (Fig. 3C and D). At this time-point after IONC, injured retinas showed no signs of axonal degeneration close to the optic disk (Fig. 3E), but in the peripheral retina there were numerous cell bodies exhibiting various degrees of RT97 staining (Fig. 3F) as well as frequent intra-axonal accumulations of pNFH (Fig. 3G and H).

At 14 and 21 days post-injury, the abovementioned changes in the expression pattern of pNFH had evolved further and appeared more generalized throughout the retina. IONT caused a decrease in the size of the axonal bundles converging toward the optic disk to leave the retina, but such a decrease was not obvious to the naked eye after IONC. Fig. 4 shows representative examples of the central retina after IONT (Fig. 4A and B) or IONC (Fig. 4E and F) at 14 days post-injury. Representative examples of the central retina at 21 days post-injury, after IONT or IONC are shown in Fig. 5A and C respectively. These images show that after IONC, pNFH-positive cell bodies start to appear closer to the centre of the retina (Figs. 4F and 5D). After either lesion, there are clear aberrant pNFH patterns (Fig. 4B–D, F–H) ranging from highly positive cell bodies whose dendrites appear to be shrinking (Fig. 4C–H), to intra-axonal pNFH-accumulations (Fig. 4B–D) or cell bodies and dendrites clearly labelled (Figs. 5B, 4F and D). It was possible to follow single axons stained with RT97 from the optic disk towards the retinal periphery where the parent cell somata often showed also intense labelling. Some of these pNFH-positive RGCs had the appearance of a rounded RGC body with very few or none dendritic ramifications (Fig. 4G and H), probably representing a prelude of what would later become into a club or a bulb-shaped cell body structure.

By day 30 post-IONT there were few pNFH-positive axons remaining in the centre (Figs. 5E and 6B) and in the periphery of the retina where these presented varicosities, bead-like formations and frequent depositions of pNFH-positive material in the forms previously described of bulbs or clubs (Fig. 5F and G). RGC bodies and dendrites intensely labelled with RT97 were still present throughout the retina but in smaller quantities than those observed at earlier intervals. At

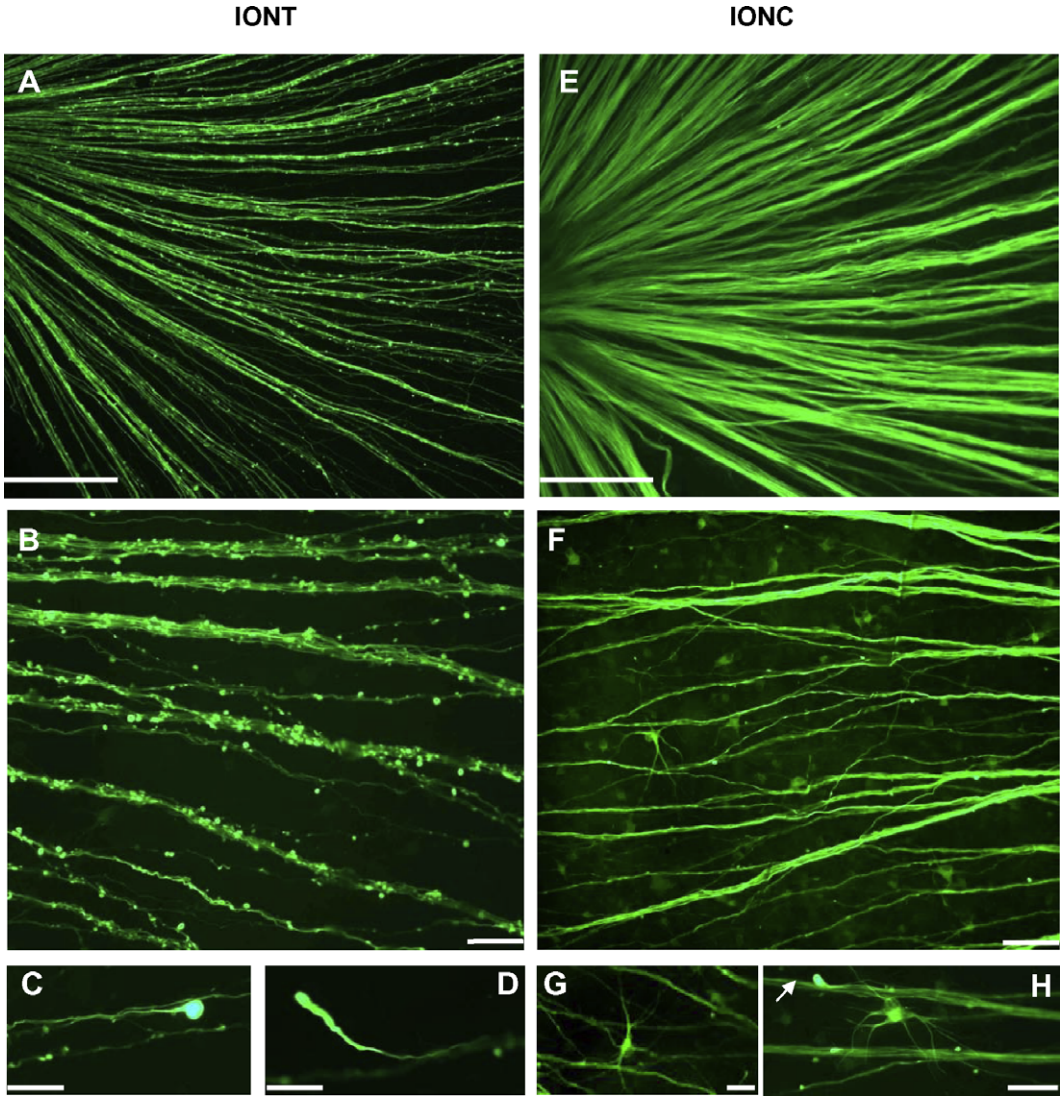

Fig. 3. Changes of the expression pattern of RT97 immunoreactivity 12 days after IONT or IONC. Twelve days after IONT the density of RGC axons pNFH-positive in the central retinas has diminished (A), but this decrease is not obvious after IONC (E). In the peripheral retina axonal degeneration continues, appearing more pNFH-accumulations and club-like axonal terminals heavily stained with RT97 after IONT (B–D) while after IONC, in addition to numerous pNFH-positive cell bodies (F–H) also axonal accumulations of pNFH start to appear (H; arrow). *Abbreviations:* IONT: intra-orbital nerve transection, IONC: intra-orbital nerve crush, pNFH: phosphorylated neurofilament heavy subunit. Bars: A, E: 200 μm, B–D, F–H: 50 μm. Top: superior, right: temporal.

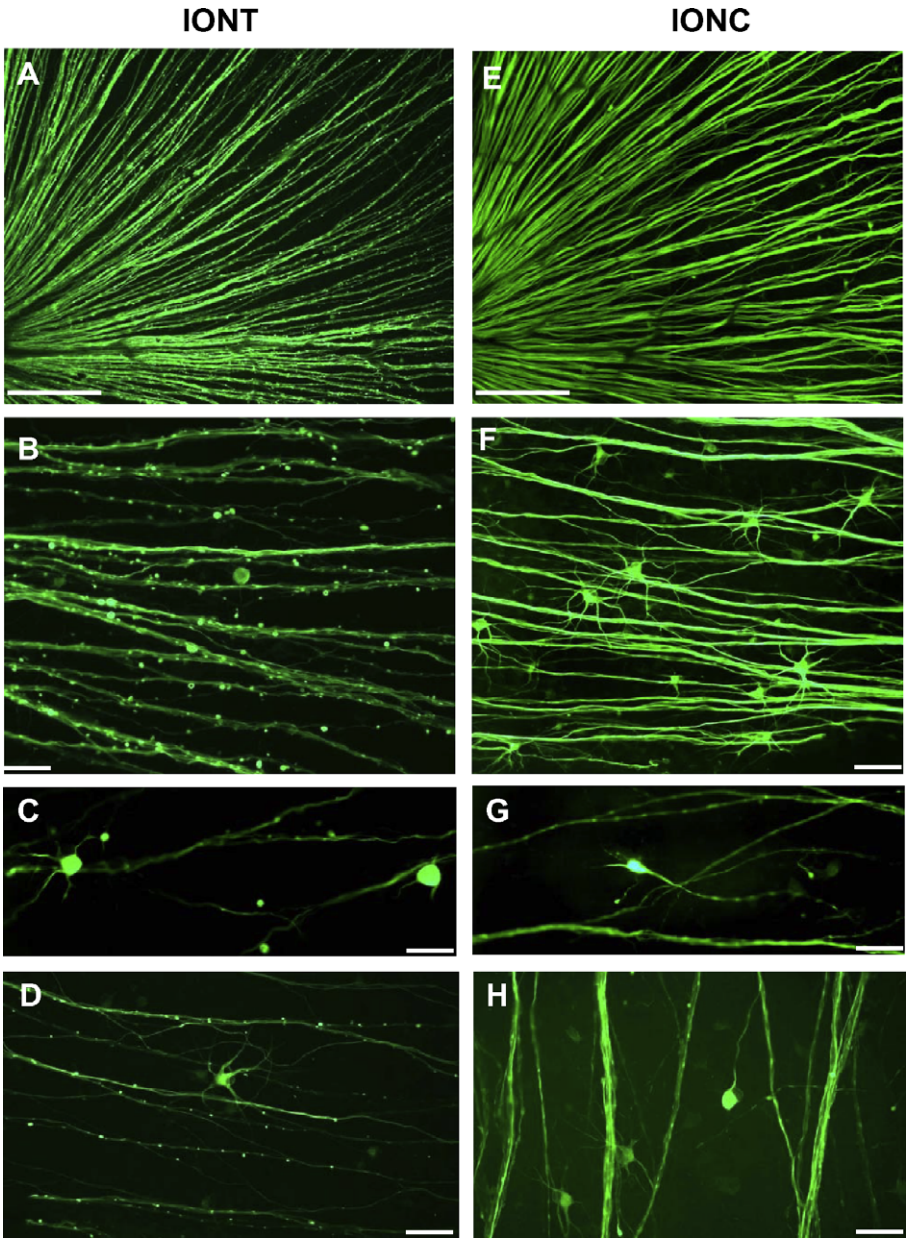

Fig. 4. Changes of the expression pattern of RT97 immunoreactivity 14 days after IONT or IONC. Fourteen days after IONT the axonal density in the centre of the retina has further diminished (A), and pNFH-aberrant accumulations are obvious (B–D) spreading from the periphery towards the middle and centre of the retina. After IONC, axonal density in the central retina has not decreased apparently (E), and in the periphery many pNFH-positive cells are observed (F), some of which had the appearance of a rounded RGC body with very few (G) or none dendritic ramifications (H), probably representing a prelude of what would later become into a club or a bulb-shaped cell body structure. *Abbreviations:* IONT: intra-orbital nerve transection, IONC: intra-orbital nerve crush, pNFH: phosphorylated neurofilament heavy subunit. Bars: A, E: 200 μm, B–D, F–H: 50 μm. Top: superior, right: temporal.

this time-point after IONC, the number of pNFH-positive axons appears to be reduced to the naked eye (Figs. 5H and 6E) and within the midperipheral retina numerous cell bodies with varying intensity of RT97 immunoreactivity as well as axons with intra-axonal pNFH-accumulations were found (Fig. 5I).

Three months after IONT, there were very few axons remaining in the centre and periphery of the retina (Fig. 6C), and most appeared faintly stained with RT97 while some presented the degenerative features described above (irregular morphology, varicosities and bead-like processes). At this time-point after IONC, there was a clear diminution in the density of axonal bundles in the central (Fig. 6F) and peripheral retina. RT97 stained RGCs were observed very seldom at this stage after either type of ON injury.

3.2. Quantitative analysis

3.2.1. Time-course emergence of pNFH-positive RGC bodies

Our qualitative analysis suggested that: (i) The number of $pNFH^+$ cells increased with time post-lesion, peaking at between 7 and 21 days; (ii) These cells were more abundant after optic nerve crush than after optic nerve transection, and; (iii) As survival interval increased there appeared to be more $pNFH^+$RGCs showing a strong RT97 staining. We have further investigated these issues by quantifying the total number of cells showing strong and faint RT97 immunoreactivity in control retinas (naïve and right eyes) and in retinas from both experimental groups at 3, 7, 14, 21 and 30 days post-IONC or IONT (graphs in Fig. 7A and B, and Table 1). RT97 immunostained RGCs were not analyzed in detail and no at-

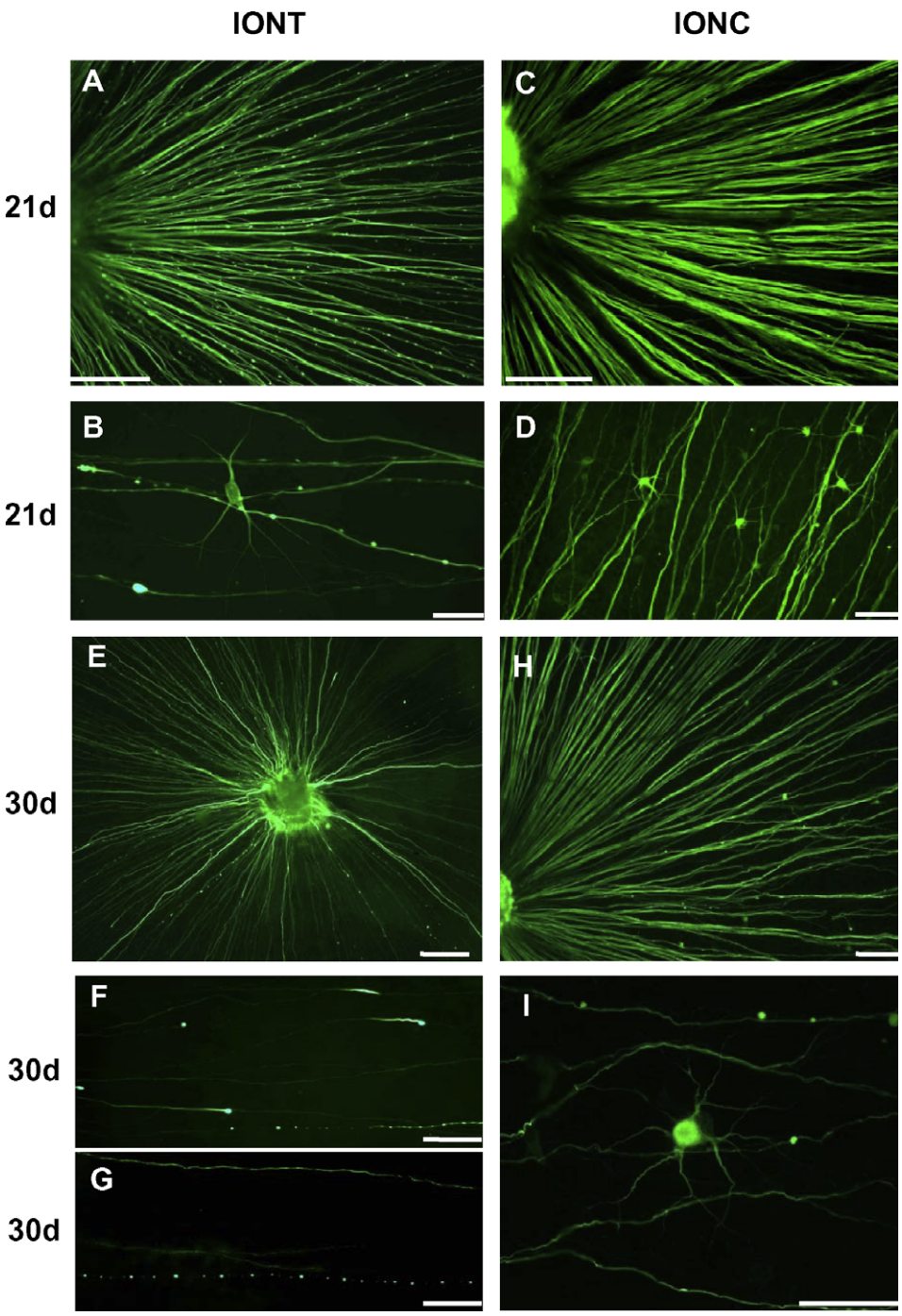

Fig. 5. Changes of the expression pattern of RT97 immunoreactivity 21 or 30 days after IONT or IONC. Twenty one days after IONT the number of RT97 positive axons in the central retina continues diminishing and pNHF accumulations spread to the optic disk (A), whereas after IONC the pNFH-expression pattern in centre of the retina has a normal looking appearance (C). Abnormal pNFH patterns after IONT are mainly axonal varicosities, although some RGC somas are also RT97 positive (B) whilst after IONC pNFH are mainly accumulated in the neuronal perikaryon and dendrites (D). Thirty days after IONT the number of RT97 axons has decreased dramatically in the centre of the retina (E) whilst at the periphery the most proximal aspects of the few remaining axons show intense RT97 staining (F), and along their length pNFH are accumulated in rosary-like beads (G). At this time-point after IONC (H) there are more pNFH-positive axons than after IONT but by this time, the axonal density has decreased compared to earlier time-points. In addition, the aberrant RT97 pattern has spread, and some pNFH-positive cells bodies are found closer to the retinal centre. In the retinal periphery abnormal expression of pNFH in the cell somas and in the axons is still present (I). *Abbreviations:* IONT: intra-orbital nerve transection, IONC: intra-orbital nerve crush, d: days post-lesion. pNFH: phosphorylated neurofilament heavy subunit. Bars: A, C, E, H: 200 μm, B, D, F, G, I: 50 μm. Top: superior, right: temporal.

tempt was made to classify these neurons on the basis of their soma size or dendritic appearance.

In the four naïve control retinas analyzed, there was a total of only three pNFH$^+$RGCs, a number that does not differ from that found in the right eyes analyzed ($n = 8$) where five pNFH$^+$RGCs were found. However, at 3 days after axotomy the total mean number ± SEM of RT97$^+$ cells was 217 ± 143 or 220 ± 126 after IONC or IONT respectively, wherein most of them showed a faint RT97 immunostaining. These values were significantly higher than control ones (Mann Withney test $p = 0.016$ for IONC 3 d *vs* control and $p = 0.036$ for IONT 3dpl *vs* control) (Fig. 7A and B, white *vs* black bars). At 7 days the total mean number ± SEM of RT97$^+$RGCs had increased to 629 ± 196 or 391 ± 129 after IONC or IONT, respectively. Fourteen days after both lesions, the total number of RT97$^+$RGCs

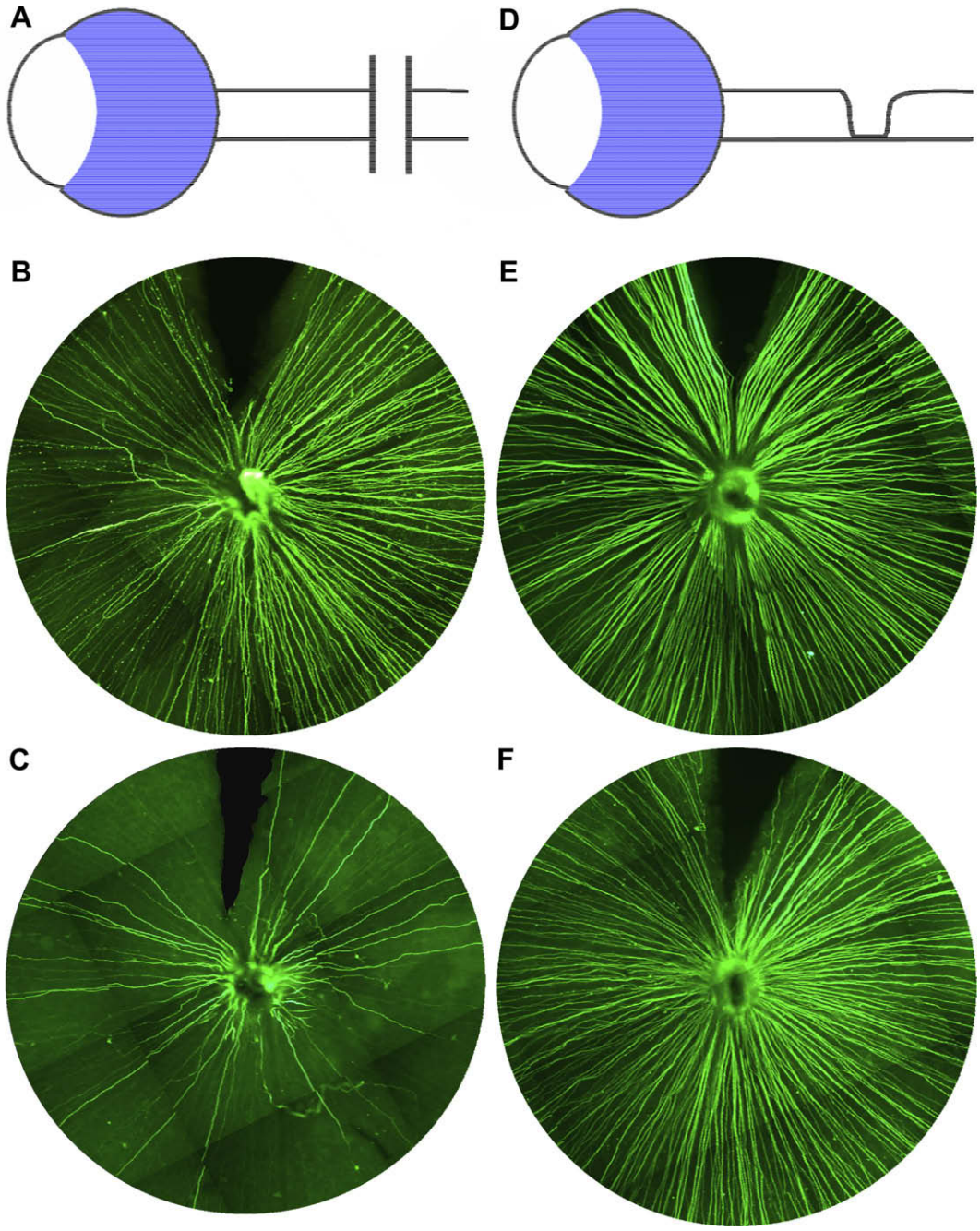

Fig. 6. Axonal degeneration is quicker after IONT than after IONC. Schematic drawings depicting optic nerve injury at approximately 3 mm from the optic disk by IONT (A) or IONC (D). B, E. Representative micrographs illustrating RT97 immunoreactivity in the central retina 30 days post-IONT (B) or IONC (E), respectively. C, F: Representative micrographs illustrating RT97 immunoreactivity in the central retina 90 days post-IONT or IONC, respectively. Notice that at the same time-point after axotomy, there are less RT97 positive axons after IONT than after IONC. *Abbreviations:* IONT: intra-orbital nerve transection, IONC: intra-orbital nerve crush, d: days post-lesion. Top: superior, right: temporal.

reached its peak, with an average of 961 ± 324 or 493 ± 188 cells after IONC or IONT (Fig. 7B and D, black bars). At 21 and 30 days post-lesion, there were approximately the same total mean number of RT97$^+$RGCs (381 ± 195 and 432 ± 152 after IONC or 242 ± 140 and 392 ± 123 after IONT, respectively). The number of pNFH$^+$RGCs counted at 14 days post-IONC is significantly higher than that at 3 or 30 dpl (Mann Withney test, IONC 3 d *vs* IONC 14 d $p = 0.026$; IONC 14 d *vs* IONC 30 d $p = 0.004$). However, there is not a significant difference for the number of cells counted after IONT at these time-points.

There is a high variability among retinas regarding their total number of RT97$^+$RGCs, which is evident when looking at the maximum and minimum number of these cells counted in individual retinas (see Table 1). In spite of this variability, three main conclusions can be reached: (i) there is a clear trend towards more pNFH$^+$RGCs after IONC than after IONT and this is evidenced at its peak time-point, 14 dpl, when the difference is significant (Mann Whitney test, $p = 0.039$), (ii) pNFH$^+$RGCs appear as early as 3 days post-lesion, their number peaks at 14 days, diminishing by 21 and 30 dpl, and; (iii) At all time-points examined, the vast majority of the pNFH$^+$ cells showed a low RT97 immunoreactivity. The number of intensely labelled RGCs increased from 3 days onwards, peaking at 14 days.

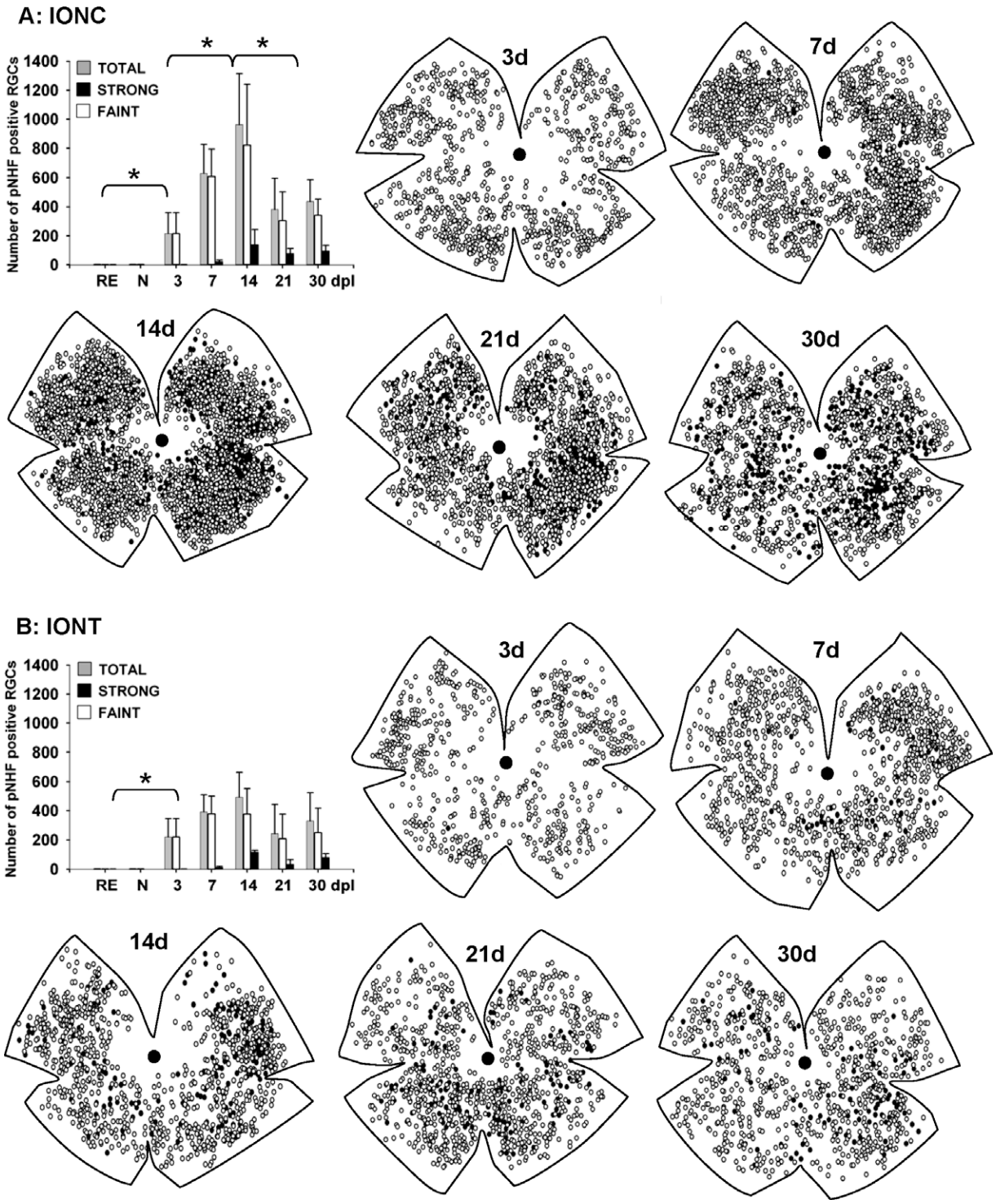

Fig. 7. Number and spatial distribution of pNFH-positive RGCs after IONC or IONT. Histograms showing mean (±SEM) total numbers of pNFH-positive RGCs at different survival intervals after IONC after IONC (A) and after IONT (B). *Mann Whitney test $p < 0.05$ (see text). Drawings depicting the location of pNFH-positive RGCs in the retina after IONC (A) or IONT (B). These drawings where generated by representing the pooled number of pNFH RGCs in three representative retinas per lesion and time-point analyzed (for details see material and methods). The retinal perimeters were manually drawn from the original analyzed retinas, adjusting them to encircle all the positive cells. In agreement with the time-course graphs, the number of pNFH-positive RGCs increases with time, peaking at day 14 post-lesion. At day 3 post-lesion most pNFH$^+$RGCs, which are weakly stained (white bars and open circles), appear on the periphery and middle retina. As time evolves more pNFH$^+$RGCs appear occupying the middle and central retina, reaching its peak by 14dpl. At this time-point pNFH$^+$RGCs strongly stained reach its maximum (black bars and black circles). From 14 days onward the number of pNFH$^+$RGCs decreases. Black bars and black circles correspond to pNFH$^+$RGCs strongly stained (as that marked with an arrow in Fig. 7C) and white bars and open circles to pNFH$^+$RGCs weakly stained (as that marked with an asterisk in Fig. 7D). All retinas are orientated with the superior pole at 12 o'clock (as drawing in Fig. 9D).

3.2.2. pNFH-positive cell bodies are degenerating axotomized RGCs

One of the characteristic features associated with optic nerve injury is the presence of cells bodies and dendrites labelled with RT97 and thus pNFH$^+$. To assess whether these cells were in fact degenerating RGCs and not other RGC layer neurons, we applied two retrograde tracers DTMR or FG to the ocular stump of the op-

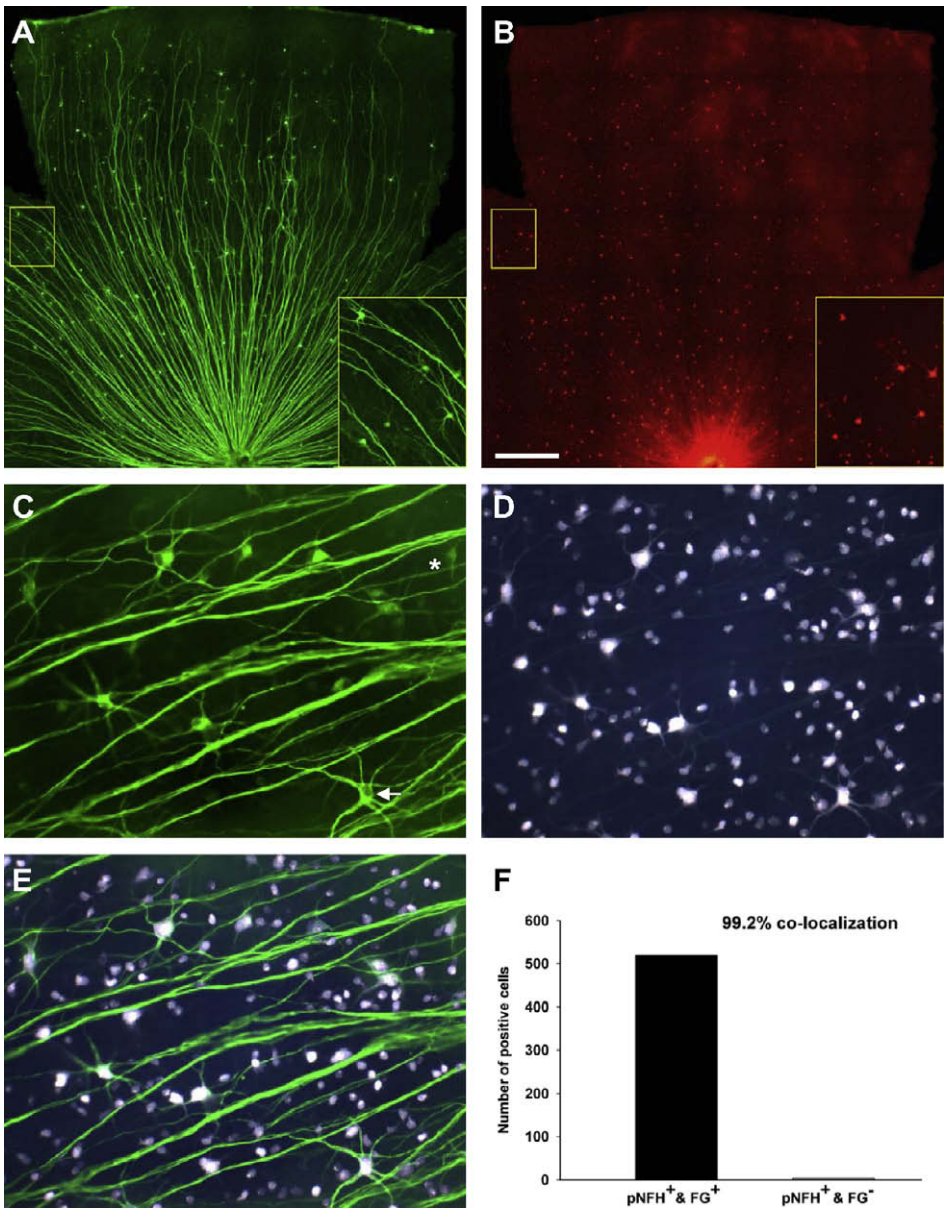

Fig. 8. pNFH-positive cells are degenerating retinal ganglion cells. Representative illustration of the inferior temporal quadrant of a retina examined 30 days after IONC immunoreacted for RT97 (A). Forty eight hours prior to processing, surviving RGCs were identified with the fluorescent retrograde tracer dextran tetramethylrhodamine (DTMR) applied to the optic nerve (B). Upon careful examination under the fluorescence microscope, every pNFH-positive cell (A) was also doubly labelled with DTMR (B), indicating that axotomy-induced RGC degeneration courses with an abnormal pNFH-accumulation in the somata of RGCs but not in other retinal neurons. A magnified area from the top-left square is shown in the bottom-right insert. In another group of animals 14 days after IONC fluorogold was applied to the optic nerve stump for three days. In these retinas, there were many pNFH-positive somas (C) and these are RGCs, as all of them co-localize with fluorogold, (D, coupled in E). F: Graph showing the number of pNFH somas that were also FG positive (black bars). In seven retinas we examined 520 retinal neurons that were $pNFH^+$, and 516 were also retrogradely labelled with FG and four were not (grey bar), which represents a 99.2% of co-localization. *Abbreviations:* IONT: intra-orbital nerve transection, IONC: intra-orbital nerve crush. Bars: 300 μm. Arrow indicates an RGC showing strong pNFH-signal and asterisk a faint one.

tic nerve. DTMR, once applied, diffuses retrogradely filling axons and their RGC soma, whilst FG is actively transported. In the DTMR labelled group of animals, a careful examination under the fluorescence microscope with both filters revealed that every RGC labelled with RT97 (Fig. 8A) was also doubly labelled with DTMR (Fig. 8B), but not vice versa, thus documenting that RT97 labelled neurons observed in the RGC layer after IONC represent RGCs and no other type of retinal neurons. As observed with DTMR; fluorescence microscropy examination of the RT97 and FG labelled retinas suggested that the vast majority of $pNFH^+$ cells were also FG^+ (Fig. 8C–E) but again, not vice versa. To assess quantitatively whether the majority of $pNFH^+$ cells were FG-traced RGCs, we counted a total of 524 $pNFH^+$ cells in individual frames of 7 retinas ($n = 8$ frames per retina). Out of them, 520 were also FG positive, thus demonstrating that 99.2% of the RT97 positive somas are RGCs (Fig. 8F). These results provide additional direct evidence to previous studies indicating that axotomy-induced RGC degeneration courses with an abnormal pNFH-accumulation in the RGC somata (Marco-Gomariz et al., 2006; Salinas-Navarro et al., submitted for publication; Vidal-Sanz et al., 1987; Villegas-Pérez et al., 1988; Villegas-Pérez et al., 1996; Villegas-Pérez et al., 1998; Wang et al., 2000; Wang et al., 2003).

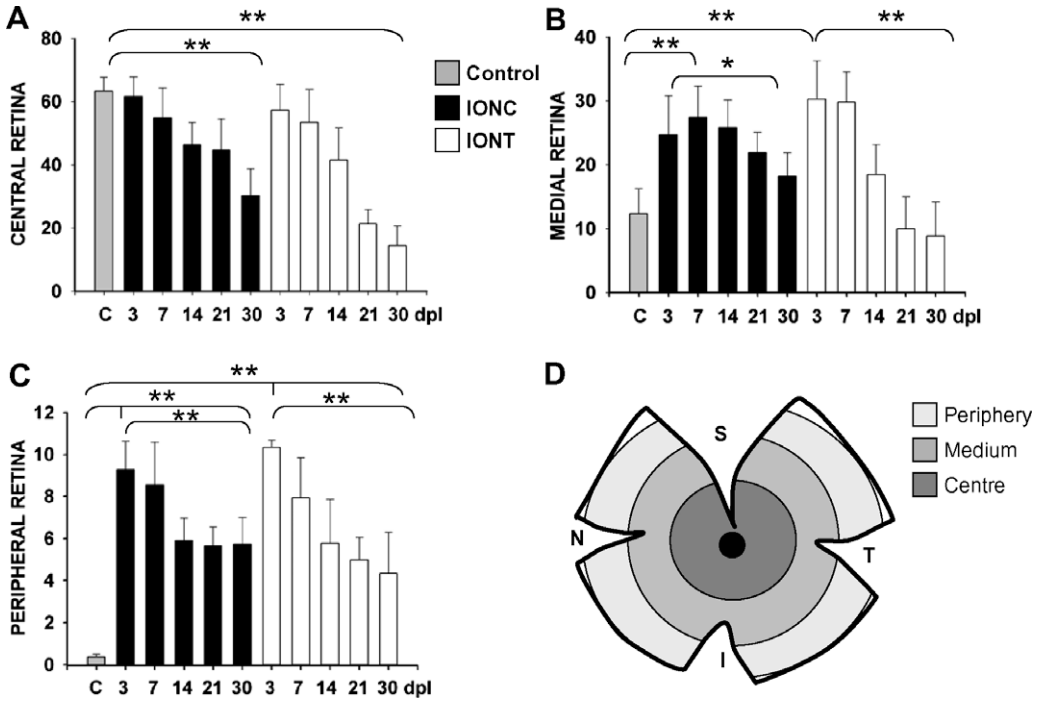

Fig. 9. pNFH-expression pattern changes after IONC and IONT. A-C Histograms showing the percentage of the central (A), medial (B) and peripheral (C) retinal area positive for pNFH immunofluorescence. The analyzed retinal areas are shown in D and their total area was considered 100% (for details see material and methods). *Mann Whitney test $p < 0.05$; **Mann Whitney test, $p < 0.001$ (see text). In the central retina, pNFH immunofluorescence decreases with time after either lesion (A). In the medial retina, there is an increase of pNFH immunofluorescence that peaks between 3 and 7 days post-IONC or IONT, decreasing afterwards after IONT (B, white bars) or IONC (B, black bars). pNFH immunofluorescence in the peripheral retina is very low in control retinas (C, grey bar), however at 3 days after IONC (C, black bars) or IONT (C, white bars) there is a clear increase of the RT97 immunofluorescence which remains above control values till 30 days post-lesion. *Abbreviations*: S: superior pole, T: temporal pole, I: inferior pole, N: nasal pole.

3.2.3. Spatial distribution of pNFH$^+$RGCs after IONT and IONC

To assess the notion, observed in the qualitative studies, that pNFH$^+$RGCs spread centripetally, appearing first at the retinal periphery and later closer to the optic disk, we examined their spatial distribution for each of the counted retinas. Even though there were some inter animal variability within each of the subgroup of retinas, the conclusions can be drawn from a graphic representation of the pooled data from three representative retinas in each group (Fig. 7A and B). Positive pNFH$^+$RGCs were distinguished according to their pNFH intensity into faint (open circles) or strong (black circles). Examination of these graphics allows to draw at a first glance three main conclusions: (i) There are more pNFH$^+$RGCs after IONC and IONT (compare Fig. 7A with B at any time-point); (ii) The pNFH$^+$RGCs are distributed throughout the whole retinal surface, in what appears a random manner, i.e. there is not a specific retinal quadrant or retinal region with greater numbers, and; (iii) The total numbers of pNFH$^+$RGCs increases with increasing survival intervals, reaching a maximum at 14 d post either injury; this is very obvious after IONC where these cells heavily populate the whole retina. A more detailed observation discloses that at 3 dpl these cells are more abundant in the medial and peripheral retina but as time post-lesion increases, there are more RT97$^+$RGCs closer to the optic disk. Moreover, at our earliest time-point examined, which was 3 dpl, pNFH$^+$RGCs show a faint RT97 staining (open circles), and this grade of staining is the more abundant throughout the study. At 7 dpl, some cells, mainly in the temporal retina, start to show a strong RT97 staining (black circles). At day 14, heavily stained RGCs reach their maximum and are spread thorough the retina, although there appears to be a certain trend for strongly RT97 immunoreactive cells to be more abundant in the temporal retina, as previously suggested for the axotomized mice retina (Drager and Hofbauer, 1980). At 21 and 30 days, pNFH$^+$RGCs distribute themselves over the entire retinal surface, but in lower numbers.

3.2.4. Temporal and spatial changes of axonal pNFH-expression pattern after IONT and IONC

In naïve retinas from intact animals, as well as in the contralateral fellow retinas of injured animals, pNFH axonal expression pattern is mainly restricted to the centre of the retina. After IONT or IONC this pattern changes and axons in the medial and peripheral retina appear immunolabelled with RT97. We have quantified in control and experimental retinas the area occupied by pNFH fluorescence in these three retinal regions (Fig. 9). The data show that in control naïve retinas pNFH$^+$ axons occupy a 61 ± 3% of the central area, in the medial area this surface drops to a 13 ± 3% and in the periphery only a 0.37 ± 0.15% of the area is RT97$^+$. These percentages do not differ from those found in the eight control right eyes analyzed (61 ± 4%, 12 ± 4% and 0.36 ± 14% for the central, medial and peripheral retina, respectively).

However, this pattern changes after both injuries, and so in the centre of the retina (Fig. 9A) the pNFH$^+$ area diminishes with time post-lesion. There is a significant trend towards diminution, that reaches its peak by 30 days after IONC or IONT, the longer survival interval quantified in this study, when only 30 (Mann Withney test, $p \leqslant 0.001$) or 14% (Mann Withney test $p \leqslant 0.001$) of the central area, respectively, is RT97$^+$.

This situation is very different in the middle and peripheral retina. For instance in the middle region pNFH$^+$ immunoreactivity accounts for 14% in the normal retina, but by 3 dpl there is an abrupt and significant increase in pNFH immunoreactivity (24% and 30% after IONC and IONT, respectively. Mann Withney test $p \leqslant 0.001$ for both lesions). This immunoreactivity peaks at day 7, diminishing then gradually up to day 30 below control values after IONT but

Table 1
Number of pNFH$^+$RGCs along time after IONT and IONC. Number of pNFH$^+$ cells counted in na, control right eyes and at 3, 7, 14, 21 and 30 days post-IONC or IONT. It is shown the mean number ± the standard error of the mean (SEM) of strong and faintly positive pNFH$^+$ counted in each experimental group, as well as the total number ± SEM of these cells. Besides, because there is a high variability it is shown the maximum (max) and minimum (min) number of these cells counted in an individual retina of each group.

		RE $n = 8$			Naïve $n = 4$		
		Strong	Faint	Total	Strong	Faint	Total
Mean ± SEM		0.25 ± 0.44	0.25 ± 0.27	0.62 ± 046	0 ± 0	0.75 ± 0.37	0.75 ± 0.37
Max		1	1	1	0	1	1
Min		0	0	0	0	0	0
	IONC						
	3 d $n = 4$		7 d $n = 4$	14 d $n = 8$	21 d $n = 6$	30 d $n = 8$	
	Strong Faint Total		Strong Faint Total	Strong Faint Total	Strong Faint Total	Strong Faint Total	
Mean ± SEM	0.25 ± 0.37 217 ± 143 217.2 ± 142.75		21.75 ± 9.6 607.7 ± 186.7 629.5 ± 196	143.6 ± 103.6 820.7 ± 420.3 961.4 ± 352.8	76.3 ± 38 304.8 ± 197.5 381.1 ± 214.9	95.5 ± 41.4 341.4 ± 110.7 436 ± 149.1	
Max	1 461 461		41 943 964	400 2293 2302	130 896 1026	210 20 668	
Min	0 67 67		12 418 431	56 235 437	10 135 145	20 181 224	
	IONT						
	3 d $n = 4$		7 d $n = 8$	14 d $n = 8$	21 d $n = 5$	30 d $n = 5$	
	Strong Faint Total		Strong Faint Total	Strong Faint Total	Strong Faint Total	Strong Faint Total	
Mean ± SEM	0.33 ± 0.44 220.3 ± 125.7 220.6 ± 125.5		12.6 ± 7.4 378.5 ± 122.5 391.1 ± 119.4	117 ± 12 376.1 ± 176.6 493.1 ± 171.8	33.2 ± 31.8 209 ± 168.4 242.2 ± 200.2	80.2 ± 25.8 249.6 ± 167.9 329.8 ± 193.7	
Max	1 409 409		27 689 689	144 680 824	90 505 561	126 482 583	
Min	0 116 116		0 254 284	81 116 237	2 33 35	50 78 140	

not after IONC where this value is slightly higher than in control retinas, an 18% (Fig. 9B), and significantly lower than at 3 or 7 dpl (Mann Withney $p = 0.006$ for IONC and $p \leqslant 0.001$ for IONT).

In the periphery there is an evident and significant increase in the area occupied by pNFH$^+$ axons, where the highest values are found at day 3 post-lesion, (9% and 10% after IONC and IONT, respectively, Mann Withney test $p \leqslant 0.001$ for both lesions). From day 7 till 30 after IONT, the pNFH$^+$ area decreases (7.9%, 5.7% and 4.9%, 4.3% at 7, 14, 21 and 30 dpl). This decrease is significantly lower at 30 days than at 7 days (Mann–Whitney test $p \leqslant 0.001$) but is still significantly higher than in control retinas (Mann Withney $p < 0.006$ at 30 days post-IONT *vs* control) 7 days after IONC, pNFH$^+$ area is similar to the one at 3 dpl (8.5%), afterwards drops and is constant till the latest time-point analyzed (5.9%, 5.6% and 5.7% at 14, 21 and 30 dpl), again theses values are significantly lower at 30 days than at 7 (Mann Whitney test $p = 0.009$) but higher than control ones (Mann Withney test, $p \leqslant 0.003$, 30 days post-IONC *vs* control) (Fig. 9C). These data demonstrate that changes in the expression pattern of pNFH are an early event associated with optic nerve injury that is maintained up to 90 days post-lesion.

4. Discussion

Here we show, quantitative and quantitatively, that optic nerve injury results in abnormal expression of pNFH within axons and RGCs somas. Changes in pNFH-expression pattern are early events of axotomy-induced RGC degeneration that last, at least, up to 90 days post-injury. Three pNFH-aberrant patterns were observed upon optic nerve injury: (i) pNFH-expression in peripheral and medial axons, while in the centre of the retina pNFH-signal decreases with time earlier after IONT than IONC, thus evidencing that IONT induces a quicker degeneration than IONC; (ii) pNFH intra-axonal accumulations like varicosities, which are more abundant after IONT than IONC, and; (iii) pNFH-expression in RGCs somas, an event that is more abundant after IONC than IONT. We also demonstrate that these pNFH$^+$RGCs first appear in the peripheral and middle retina spreading towards the optic disk and are not confined to any retinal quadrant but rather spread throughout the retinal surface.

4.1. pNFH-expression in injured RGCs

In agreement with previous studies the pattern of pNFH-expression in control uninjured retinas shows RT97 staining of intrarretinal axons but not at their most proximal portion, neither in the soma nor in dendrites of the RGCs (Drager & Hofbauer, 1984; Nixon, Lewis, Dahl, Marotta, & Drager, 1989; Vidal-Sanz et al., 1987; Villegas-Pérez et al., 1988, 1996, 1998; Wang et al., 2000, 2003). In contrast, injured retinas display an abnormal expression of pNFH in the proximal portion of the intraretinal axon as well as within a variable number of cell somata and dendrites. A common feature of IONT- and IONC-induced axonal degeneration is that it appears first in the retinal periphery spreading towards the optic disk (see Figs. 7 and 9), and this is in agreement with the notion that axotomy-induced axonal degeneration starts at or near the cell body and progresses somatofugally, in a similar fashion to that reported for sciatic nerve crushed lumbar sensory neurons (Hoffman et al., 1987) and for axotomized cat RGCs (Silveira, Russelakis-Carneiro, & Perry, 1994).

Neurons showing RT97 immunoreactivity within their soma and dendrites were indeed injured RGCs and not other neurons in the RGC layer. This was demonstrated in two experimental groups of IONC-injured retinas with RGCs retrogradely labelled with DTMR or FG, respectively. In both cases, practically all RT97$^+$ cells were also doubly labelled with DTMR or FG. Our quantitative study shows some variability in the total number of RT97$^+$RGCs within

animals of specific group, but also documents that practically all RT97$^+$ stained retinal neurons are injured RGCs. Indeed the co-localization of RT97 with FG in backlabelled RGCs is almost 100%. Because upon IONT or IONC, RGCs express pNFH in their cell somas, RT97 immunostaining could be used as a marker for injured RGCs. Indeed, a recent study in which ocular hypertension induced sectorial damage to the retina documented that pNFH-expression was mainly observed within the damaged sectors while it was absent from other regions of the retina (Salinas-Navarro et al., submitted for publication). Another matter is how many of the original 82,818 RGCs present in a normal adult SD rat retina (Salinas-Navarro, Mayor-Torroglosa, et al., 2009, Nadal-Nicolás, et al. 2009) show abnormal RT97 immunoreactivity within their soma after optic nerve lesion. In our best case, which was a retina examined at 14 days after IONC, there were a total of 2302 RT97$^+$RGCs and this represents little more than 2.8% of the original RGC population. Thus, as previously suggested RT97 only identifies a small subset of RGCs (Drager & Hofbauer, 1984) disconnected from their targets (Dieterich et al., 2002; Salinas-Navarro et al., submitted for publication; Soto et al., 2008). It remains to be further investigated whether these RT97$^+$RGCs belong to a specific type of RGCs.

pNFH-expression in the cell soma and dendrites displays a variable degree of intensity, ranging from a faint but clear labelling to a golgi-like staining (Figs. 3B and H, 4F, 7 and 8). The chronology of our observations tempts us to speculate that faint and strong RT97 immunoreactivity within RGCs correspond to early and late stages of RGC degeneration, respectively. This is clearly observed when looking at their spatial distribution along the time (Fig. 7). At early time-points after ON injury, most of the pNFH$^+$RGCs show a low RT97 staining and they are located in the peripheral and middle retina, but as the survival interval progresses RGCs highly pNFH$^+$ start to appear and both, high and low RT97$^+$RGCs, are found closer to the optic disk. Moreover, RGCs showing clear signs of degeneration, such as those illustrated in Figs. 3C and D or 4C, G and H or 5F, are strongly immunoreactive.

This study shows that these cells are not spatially confined to any retinal quadrant but they rather appear on the periphery and middle retina, quickly distributing over the whole retinal surface including the central retina (see Fig. 7). These findings might appear to be at odds with a general rule in the primary visual pathway that says that the closer the site of axotomy to the RGC somata, the most severe the RGC loss is (Villegas-Pérez et al., 1993). While the latter is true, the assertion is based on counts of the RGC population as a whole, which as mentioned earlier it is several orders of magnitude greater than the population of injured RGCs that become stained with RT97. Nevertheless, the observation that RT97$^+$RGCs are distributed throughout the retina is also in agreement with our recent spatial analysis of RGC loss after IONT or IONC (Nadal-Nicolás et al., 2009) indicating that ON axotomy-induced RGC death is diffuse and affects the whole retina.

4.2. Different pattern and time-course of abnormal pNFH-expression after IONT or IONC

We have described in the RGC fibre layer the degenerative changes induced by two types of complete optic nerve injury, transection or crush, performed at approximately the same distance from the eye. Abnormal pNFH-expression is associated with a number of degenerative events that take place in the RGC soma, its primary dendrites and intraretinal axons, eventually leading to degeneration of these neurons. Although similar events can be found in both situations, there were some differences in the pattern and time-course of axonal degeneration among both injuries (summarized in Table 2): (i) accumulations of pNFH in the cell soma and dendrites were more frequently observed after IONC than IONT (Fig. 7) and conversely, intra-axonal varicosities were more frequently observed after IONT than IONC; (ii) the abnormal intra-axonal accumulations of pNFH appear quicker after IONT than after IONC, and; (iii) after IONT the number of RGC axons identified by RT97 immunoreactivity decreases quicker than after IONC (Figs. 6 and 9). In other words, the severity and time-course of axonal degeneration within the nerve fibre layer of the retina is greater and quicker after IONT than after IONC, and this is in agreement with previous reports showing that IONT induces a quicker and more severe RGC degeneration than IONC (Agudo et al., 2008, 2009).

Abnormal pNFH patterns were observed at high magnification as early as 3 dpl when pNFH$^+$ axons were observed in the medial and peripheral retina (Figs. 2 and 9). After IONT, RGC axons exhibit a varicose morphology, with the apparition of rosary-like beads along them. Often, the most proximal portion of the axon ended in club- or bulb-like shaped bodies, which most likely represent an advanced stage of RGC degeneration. After IONC however, pNFH-aberrant signal was mainly observed in RGC bodies and dendrites and this pattern also progressed with time to RGCs highly pNFH-positive with shrinking dendrites (see Figs. 4G and H, and 7) also suggesting an evolving state of RGC degeneration. These observations are in agreement with previous reports (Dieterich

Table 2
Summary of the changes of pNFH-expression occurring after IONC and IONT. Expression of pNFH is ranged from highest (+++++) to lowest (–) in terms of retinal area occupied by pNFH-signal (axonal expression of pNFH in the central, medial or peripheral retina) or number of axonal varicosities or pNFH$^+$RGCs found in control (0 days) and in IONC or IONT-injured retinas along time post-lesion.

		Control (0d)	3d	7d	14d	21d	30d
Axonal expression of pNFH	Central	+++++	IONC: +++++	++++	++++	+++	+++
			IONT: +++++	++++	+++	++	+
	Medial	++	IONC: ++++	++++	++++	+++	+++
			IONT: +++++	+++++	+++	++	+
	Peripheral	-	IONC: +++++	++++	+++	+++	+++
			IONT: +++++	++++	+++	++	++
Axonal varicosities		-	IONC: -	+	++	+	+
			IONT: -	++	+++++	++++	++
pNFH$^+$RGCs	Strong	-	IONC: -	+	+++++	+++	+++
			IONT: -	+	++++	+	++
	Faint	-	IONC: +	++++	+++++	++	++
			IONT: +	++	++	+	+

et al., 2002) describing pNFH-accumulation in the cytoplasm of RGCs that have undergone complete axotomy.

Regarding the time-course of axonal degeneration, axonal loss appears earlier after IONT than IONC. At low magnification axonal loss was not evident until day 12 after IONT or until day 30 after IONC, in agreement with our quantitative analysis (Fig. 9) that shows that RT97 immunoreactivity in the central retina decreases earlier and more severely after IONT than IONC. This is further supported in the study of injured retinas at three months post-lesion, where it is observed that after IONT, but not after IONC, very few axons remain in the retina (Fig. 6C and F). This is consistent with recent studies in which it was demonstrated that RGC degeneration is quicker when the ON is transected than when is crushed (Nadal-Nicolás et al., 2009; Parrilla-Reverter et al., 2009; Peinado-Ramon et al., 1996), and might be a reflection of the different transcriptional regulation that has been reported in retinas undergoing either type of injury (Agudo et al., 2008; Agudo et al., 2009). The different number of pNFH$^+$RGCs observed after IONC or IONT, at similar survival intervals, might be explained because IONT induces a more severe and rapid RGC loss than IONC. Alternatively, IONC or IONT may elicit a different pNFH-expression in individual RGCs. Indeed, the expression of *NF* mRNAs is quickly down-regulated in the retina after IONT or IONC (Agudo et al., 2008; Hoffman et al., 1993; McKerracher, Essagian, & Aguayo, 1993). This reduction in *NF* expression, which is considered a general neuronal response to axonal injury (Hoffman et al., 1993) correlates as well, with a slowed down axonal transport of cytoskeletal proteins and a decrease in the amount of NF protein transported (McKerracher, Vidal-Sanz, Aguayo, 1990; McKerracher, Vidal-Sanz, Essagian, et al., 1990).

4.3. Mismatch between RGC fibre layer appearance and number of surviving RGCs

The present studies utilize qualitative and quantitative techniques to identify the RGC axons in the nerve fibre layer of the retina. Our results highlight the difficulties in assessing the degree of RGC survival based on observations of the RGC fibre layer, because the loss of RGC axons in the fibre layer only appears evident at stages in which the neurodegenerative process of the RGC population is very advanced. In other words, axonal loss is only apparent at 12 or 14 days after IONT (see Figs. 3C, 4A and 9), a time when quantitative studies have documented that approximately less than 20% of the RGC population survive in the retina (Parrilla-Reverter et al., 2009; Peinado-Ramon et al., 1996; Villegas-Pérez et al., 1993). In the case of IONC, it was not until 21–30 days after the injury (Figs. 5H and 6D) that examination of the RGC fibre layer denoted a clear diminution in the number of axons, a time when quantitative studies have estimated that approximately less than 20% of the RGC population survive in the retina (Berkelaar et al., 1994; Parrilla-Reverter et al., 2009). Thus, as previously suggested (Salinas-Navarro et al., 2008), these observations indicate that imaging the retinal nerve fibre layer with neurofilament staining is not a reliable index of the amount of RGC survival. Indeed, our quantitative analysis indicates that 30 days after lesion, within the central retina RT97 immunoreactivity diminishes from 61% in control to 30% in IONC retinas and to 14% in IONT retinas. In other words, the immunofluorescence elicited by RGC axons in the central retina diminished to one half or to one quarter, for IONT or IONC, respectively, and these do not match the corresponding diminutions in the RGC population to approximately less than 10% or 20% after IONT or IONC, respectively.

4.4. Final comments

Altogether, the present study indicates that RT97 immunoreactivity is a good technique to assess, even at early time-points, whether a given retina is undergoing a pathological process associated with axonal injury by looking at its pNFH abnormal axonal or cellular expression (Salina-Navarro et al., submitted for publication). Furthermore, our quantitative analysis provides for the first time, the maximum, minimum and mean number of pNFH$^+$RGCs after IONT or IONC, and these data might be useful to correlate different retinal diseases with a crush or transection-like temporal course of degeneration. Finally, our results further strengthen the different biological responses elicited on RGCs after two types of ON injury. In this work both IONC and IONC were performed at the same distance from the optic disk, thus being comparable in terms of disconnection of the cell soma from its main target territories in the brain. These two injuries however, trigger different responses in the RGC population which are already present shortly after the insult at the molecular level (Agudo et al., 2008; Agudo et al., 2009), result in different rates of RGC loss (Nadal-Nicolás et al., 2009; Parrilla-Reverter et al., 2009; Peinado-Ramon et al., 1996) and may be also responsible for the different intensity and cadence of these degenerative events, as visualized with a neurofibrillar staining.

Acknowledgments

The authors would like to thank Sergio Mayor for his technical assistance with the illustrations, and Isabel Cánovas-Martínez and Leticia Nieto-López for their expert technical support. This work was supported by research grants from the Regional Government of Murcia, Fundación Séneca 02989/PI/05, 05703/PI/07, 04446/GERM/07; Spanish Ministry of Education and Science SAF-2005-04812; and Spanish Ministry of Health and ISCIII-FEDER: CP003/00119; PIO70225; PIO06/0780 and RD07/0062/0001.

References

Agudo, M., Pérez-Marín, M., Lönngren, U., Sobrado, P., Conesa, A., Cánovas, I., et al. (2008). Time course profiling of the retinal transcriptome after optic nerve transection and optic nerve crush. *Molecular Vision, 14*, 1050–1063.

Agudo, M., Pérez-Marín, M. C., Sobrado-Calvo, P., Lonngren, U., Salinas-Navarro, M., Canovas, I., et al. (2009). Immediate upregulation of proteins belonging to different branches of the apoptotic cascade in the retina after optic nerve transection and optic nerve crush. *Investigative Ophthalmology and Visual Science, 50*, 424–431.

Al Chalabi, A., & Miller, C. C. (2003). Neurofilaments and neurological disease. *BioEssays, 25*, 346–355.

Anderton, B. H., Breinburg, D., Downes, M. J., Green, P. J., Tomlinson, B. E., Ulrich, J., et al. (1982). Monoclonal antibodies show that neurofibrillary tangles and neurofilaments share antigenic determinants. *Nature, 298*, 84–86.

Avilés-Trigueros, M., Mayor-Torroglosa, S., García-Avilés, A., Lafuente, M. P., Rodríguez, M. E., Miralles de Imperial, J., et al. (2003). Transient ischemia of the retina results in massive degeneration of the retinotectalprojection: Long-term neuroprotection with brimonidine. *Experimental Neurology, 184*(2), 767–777.

Aviles-Trigueros, M., Sauve, Y., Lund, R. D., & Vidal-Sanz, M. (2000). Selective innervation of retinorecipient brainstem nuclei by retinal ganglion cell axons regenerating through peripheral nerve grafts in adult rats. *Journal of Neuroscience, 20*, 361–374.

Bahr, M., Eschweiler, G. W., & Wolburg, H. (1992). Precrushed sciatic nerve grafts enhance the survival and axonal regrowth of retinal ganglion cells in adult rats. *Experimental Neurology, 116*, 13–22.

Balkema, G. W., & Drager, U. C. (1985). Light-dependent antibody labelling of photoreceptors. *Nature, 316*, 630–633.

Berkelaar, M., Clarke, D. B., Wang, Y. C., Bray, G. M., & Aguayo, A. J. (1994). Axotomy results in delayed death and apoptosis of retinal ganglion cells in adult rats. *Journal of Neuroscience*(14), 4368–4374.

Buckingham, B. P., Inman, D. M., Lambert, W., Oglesby, E., Calkins, D. J., Steele, M. R., et al. (2008). Progressive ganglion cell degeneration precedes neuronal loss in a mouse model of glaucoma. *Journal of Neuroscience, 28*, 2735–2744.

Burke, W., Cottee, L. J., Garvey, J., Kumarasinghe, R., & Kyriacou, C. (1986). Selective degeneration of optic nerve fibres in the cat produced by a pressure block. *Journal of Physiology, 376*, 461–476.

Cairns, N. J., Atkinson, P. F., Hanger, D. P., Anderton, B. H., Daniel, S. E., & Lantos, P. L. (1997). Tau protein in the glial cytoplasmic inclusions of multiple system atrophy can be distinguished from abnormal tau in Alzheimer's disease. *Neuroscience Letters, 230*, 49–52.

Chidlow, G., Casson, R., Sobrado-Calvo, P., Vidal-Sanz, M., & Osborne, N. N. (2005). Measurement of retinal injury in the rat after optic nerve transection: An RT-PCR study. *Molecular Vision, 11*, 387–396.

Cho, E. Y., & So, K. F. (1989). Regrowth of retinal ganglion cell axons into a peripheral nerve graft in the adult hamster is enhanced by a concurrent optic nerve crush. *Experimental Brain Research, 78*, 567–574.

Coleman, M. P., & Anderton, B. H. (1990). Phosphate-dependent monoclonal antibodies to neurofilaments and Alzheimer neurofibrillary tangles recognize a synthetic phosphopeptide. *Journal of Neurochemistry, 54*, 1548–1555.

Dieterich, D. C., Trivedi, N., Engelmann, R., Gundelfinger, E. D., Gordon-Weeks, P. R., & Kreutz, M. R. (2002). Partial regeneration and long-term survival of rat retinal ganglion cells after optic nerve crush is accompanied by altered expression, phosphorylation and distribution of cytoskeletal proteins. *European Journal of Neuroscience, 15*, 1433–1443.

Drager, U. C., & Hofbauer, A. (1984). Antibodies to heavy neurofilament subunit detect a subpopulation of damaged ganglion cells in retina. *Nature, 309*, 624–626.

Gotow, T., Tanaka, J., & Takeda, M. (1995). The organization of neurofilaments accumulated in perikaryon following aluminum administration: Relationship between structure and phosphorylation of neurofilaments. *Neuroscience, 64*, 553–569.

Hoffman, P. N., Cleveland, D. W., Griffin, J. W., Landes, P. W., Cowan, N. J., & Price, D. L. (1987). Neurofilament gene expression: A major determinant of axonal caliber. *Proceedings of the National Academy of Sciences of the United States of America, 84*, 3472–3476.

Hoffman, P. N., Pollock, S. C., & Striph, G. G. (1993). Altered gene expression after optic nerve transection: Reduced neurofilament expression as a general response to axonal injury. *Experimental Neurology, 119*, 32–36.

Johnstone, M., Goold, R. G., Fischer, I., & Gordon-Weeks, P. R. (1997). The neurofilament antibody RT97 recognises a developmentally regulated phosphorylation epitope on microtubule-associated protein 1B. *Journal of Anatomy, 191*(Pt 2), 229–244.

Ksiezak-Reding, H., Dickson, D. W., Davies, P., & Yen, S. H. (1987). Recognition of tau epitopes by anti-neurofilament antibodies that bind to Alzheimer neurofibrillary tangles. *Proceedings of the National Academy of Sciences of the United States of America, 84*, 3410–3414.

Lafuente Lopez-Herrera, M. P., Mayor-Torroglosa, S., Miralles d, I., Villegas-Pérez, M. P., & Vidal-Sanz, M. (2002). Transient ischemia of the retina results in altered retrograde axoplasmic transport: Neuroprotection with brimonidine. *Experimental Neurology, 178*, 243–258.

Lafuente, M. P., Villegas-Pérez, M. P., Mayor, S., Aguilera, M. E., Miralles de Imperial, J., & Vidal-Sanz, M. (2002). Neuroprotective effects of brimonidine against transientischemia-induced retinal ganglion cell death: A dose response in vivo study. *Experimental Eye Research, 74*(2), 181–189.

Lafuente, M. P., Villegas-Pérez, M. P., Selles-Navarro, I., Mayor-Torroglosa, S., Miralles d, I., & Vidal-Sanz, M. (2002). Retinal ganglion cell death after acute retinal ischemia is an ongoing process whose severity and duration depends on the duration of the insult. *Neuroscience, 109*, 157–168.

Leoz y Arcuate, J. (1914). Procesos regenerativos del nervio óptico y retina, con ocasión de injertos nerviosos. *Trab del lab de Invest Biol*.

Lewis, S. E., & Nixon, R. A. (1988). Multiple phosphorylated variants of the high molecular mass subunit of neurofilaments in axons of retinal cell neurons: Characterization and evidence for their differential association with stationary and moving neurofilaments. *Journal of Cell Biology, 107*, 2689–2701.

Lindqvist, N., Peinado-Ramon, P., Vidal-Sanz, M., & Hallbook, F. (2004). GDNF, Ret, GFRalpha1 and 2 in the adult rat retino-tectal system after optic nerve transection. *Experimental Neurology, 187*, 487–499.

Lindqvist, N., Vidal-Sanz, M., & Hallbook, F. (2002). Single cell RT-PCR analysis of tyrosine kinase receptor expression in adult rat retinal ganglion cells isolated by retinal sandwiching. *Brain Research Protocols, 10*, 75–83.

Mansour-Robaey, S., Clarke, D. B., Wang, Y. C., Bray, G. M., & Aguayo, A. J. (1994). Effects of ocular injury and administration of brain-derived neurotrophic factor on survival and regrowth of axotomized retinal ganglion cells. *Proceedings of the National Academy of Sciences of the United States of America, 91*(5), 1632–1636. Mar1.

Marco-Gomariz, M. A., Hurtado-Montalban, N., Vidal-Sanz, M., Lund, R. D., & Villegas-Pérez, M. P. (2006). Phototoxic-induced photoreceptor degeneration causes retinal ganglion cell degeneration in pigmented rats. *Journal of Comparative Neurology, 498*, 163–179.

Mayor-Torroglosa, S., De l, V., Rodriguez, M. E., Lopez-Herrera, M. P., Aviles-Trigueros, M., Garcia-Avilés, A., et al. (2005). Ischemia results 3 months later in altered ERG, degeneration of inner layers, and deafferented tectum: Neuroprotection with brimonidine. *Investigative Ophthalmology and Visual Science, 46*, 3825–3835.

McKerracher, L., Essagian, C., & Aguayo, A. J. (1993). Temporal changes in beta-tubulin and neurofilament mRNA levels after transection of adult rat retinal ganglion cell axons in the optic nerve. *Journal of Neuroscience, 13*, 2617–2626.

McKerracher, L., Vidal-Sanz, M., & Aguayo, A. J. (1990). Slow transport rates of cytoskeletal proteins change during regeneration of axotomized retinal neurons in adult rats. *Journal of Neuroscience, 10*, 641–648.

McKerracher, L., Vidal-Sanz, M., Essagian, C., & Aguayo, A. J. (1990). Selective impairment of slow axonal transport after optic nerve injury in adult rats. *Journal of Neuroscience, 10*, 2834–2841.

Morrison, J. C., Johnson, E. C., Cepurna, W. O., & Funk, R. H. (1999). Microvasculature of the rat optic nerve head. *Investigative Ophthalmology and Visual Science, 40*, 1702–1709.

Nadal-Nicolás, F. M., Jiménez-López, M., Sobrado-Calvo, P., Nieto-López, L., Canovas-Martinez, I., Salinas-Navarro, M., et al. (2009). Brn3a as a marker of retinal ganglion cells: Qualitative and quantitative time course studies in naïve and optic nerve injured retinas. *Investigative Ophthalmology Visual Science, 50*(8), 3860–3868.

Nixon, R. A., Lewis, S. E., Dahl, D., Marotta, C. A., & Drager, U. C. (1989). Early posttranslational modifications of the three neurofilament subunits in mouse retinal ganglion cells: Neuronal sites and time course in relation to subunit polymerization and axonal transport. *Brain Research. Molecular Brain Research, 5*, 93–108.

Parrilla-Reverter, G., Agudo, M., Sobrado-Calvo, P., Salinas-Navarro, M., Villegas-Pérez, M. P., & Vidal-Sanz, M. (2009). Effects of different neurotrophic factors on the survival of retinal ganglion cells after a complete intraorbital nerve crush injury: A quantitative in vivo study. *Experimental Eye Research, 89*(1), 32–41.

Parrilla-Reverter, G., Sobrado Calvo, P., Cánovas Martínez, I., Bernal Garro, J. M., Soro, M. I., Aguilera Meseguer, M. E., et al. (2006). Retinal ganglion cell axotomy induced by intraorbital nerve crush or optic nerve transection results in different time course degeneration and expression of neurofilaments. *Investigative Ophthalmology and Visual Science, 47*. E-Abstract 1248.

Peinado-Ramon, P., Salvador, M., Villegas-Pérez, M. P., & Vidal-Sanz, M. (1996). Effects of axotomy and intraocular administration of NT-4, NT-3, and brain-derived neurotrophic factor on the survival of adult rat retinal ganglion cells. A quantitative in vivo study. *Investigative Ophthalmology and Visual Science, 37*, 489–500.

Perrot, R., Berges, R., Bocquet, A., & Eyer, J. (2008). Review of the multiple aspects of neurofilament functions, and their possible contribution to neurodegeneration. *Molecular Neurobiology, 38*, 27–65.

Petzold, A. (2005). Neurofilament phosphoforms: Surrogate markers for axonal injury, degeneration and loss. *Journal of the Neurological Sciences, 233*, 183–198.

Ramón y Cajal, S. (1914). Estudios sobre la degeneración y regeneración del sistema nervioso. In: Hijos de Nicolás, M. Moya (Eds.), *Tomo II* (pp. 203–217).

Robinson, G. A. (1994). Immediate early gene expression in axotomized and regenerating retinal ganglion cells of the adult rat. *Brain Research. Molecular Brain Research, 24*, 43–54.

Salinas-Navarro, M., Alarcón-Martínez, L., Valiente-Soriano, F.J., Jiménez-López, M., Mayor-Torroglosa, S., & Avilés-Trigueros, M., et al. (submitted for publication). Ocular hypertension impairs optic nerve axonal transport leading to progressive retinal ganglion cell degeneration. *Experimental Eye Research*.

Salinas-Navarro, M., Jiménez-López, M., Valiente-Soriano, F., Alarcón-Martínez, L., Aviles-Trigueros, M., Mayor-Torroglosa, S., et al. (2009). Retinal ganglion cell population in adult albino and pigmented mice: A computerised analysis of the entire population and its spatial distribution. *Vision Research, 49*, 647–673.

Salinas-Navarro, M., Mayor-Torroglosa, S., Jiménez-López, M., Aviles-Trigueros, M., Holmes, T. M., Lund, R. D., et al. (2009). A computerized analysis of the entire retinal ganglion cell population and its spatial distribution in adult rats. *Vision Research, 49*, 115–126.

Salinas-Navarro, M., Napankangas, U., Turunen, J., Veijola, F., Valiente-Soriano, F., Villegas-Pérez, M. P., et al. (2008). Effects of acute increase of intraocular pressure in adult pigmented rats: Assessment of the retinal nerve fiber layer (in vivo) and the retinal ganglion cell population. *Investigative Ophthalmology and Visual Science, 9*, 90–99. E-Abstract 5480.

Salvador-Silva, M., Vidal-Sanz, M., & Villegas-Pérez, M. P. (2000). Microglial cells in theretina of Carassius auratus: Effects of optic nerve crush. *Journal of Comparative Neurology, 417*(4), 431–447. Feb 21.

Sasaki, H., Coffey, P., Villegas-Pérez, M. P., Vidal-Sanz, M., Young, M. J., Lund, R. D., et al. (1996). Light induced EEG desynchronization and behavioral arousal in rats with restored retinocollicular projection by peripheral nerve graft. *Neuroscience Letters, 218*, 45–48.

Silveira, L. C., Russelakis-Carneiro, M., & Perry, V. H. (1994). The ganglion cell response to optic nerve injury in the cat: Differential responses revealed by neurofibrillar staining. *Journal of Neurocytology, 23*(2), 75–86. Feb.

Sobrado-Calvo, P., Vidal-Sanz, M., & Villegas-Pérez, M. P. (2007). Rat retinal microglial cells under normal conditions, after optic nerve section, and after optic nerve section and intravitreal injection of trophic factors or macrophage inhibitory factor. *Journal of Comparative Neurology, 501*, 866–878.

Soto, I., Oglesby, E., Buckingham, B. P., Son, J. L., Roberson, E. D., Steele, M. R., et al. (2008). Retinal ganglion cells downregulate gene expression and lose their axons within the optic nerve head in a mouse glaucoma model. *Journal of Neuroscience, 28*, 548–561.

Sternberger, N. H., Sternberger, L. A., & Ulrich, J. (1985). Aberrant neurofilament phosphorylation in Alzheimer disease. *Proceedings of the National Academy of Sciences of the United States of America, 82*, 4274–4276.

Tello, F. (1907). La régénération dans les voies optiques. In: *Trabajos de Laboratorio en Investigación Biológica* (pp. 237–248).

Thanos, S., & Vanselow, J. (1989). Adult retinal ganglion cells retain the ability to regenerate their axons up to several weeks after axotomy. *Journal of Neuroscience Research, 22*, 144–149.

Veeranna Lee, J. H., Pareek, T. K., Jaffee, H., Boland, B., Vinod, K. Y., et al. (2008). Neurofilament tail phosphorylation: Identity of the RT97 phosphoepitope and regulation in neurons by cross-talk among proline-directed kinases. *Journal of Neurochemistry, 107*, 35–49.

Vidal-Sanz, M., Aviles-Trigueros, M., Whiteley, S. J., Sauve, Y., & Lund, R. D. (2002). Reinnervation of the pretectum in adult rats by regenerated retinal ganglion cell axons: Anatomical and functional studies. *Peripheral and Spinal Mechanisms in the Neural Control of Movement, 137*, 443–452.

Vidal-Sanz, M., Bray, G. M., & Aguayo, A. J. (1991). Regenerated synapses persist in the superior colliculus after the regrowth of retinal ganglion cell axons. *Journal of Neurocytology, 20*, 940–952.

Vidal-Sanz, M., Bray, G. M., Villegas-Pérez, M. P., Thanos, S., & Aguayo, A. J. (1987). Axonal regeneration and synapse formation in the superior colliculus by retinal ganglion cells in the adult rat. *Journal of Neuroscience, 7*, 2894–2909.

Vidal-Sanz, M., De la Villa, P., Aviles-Trigueros, M., Mayor-Torroglosa, S., Salinas-Navarro, M., Alarcón-Martínez, L., et al. (2007). Neuroprotection of retinal ganglion cell function and their central nervous system targets. *Eye, 21*, S42–S45.

Vidal-Sanz, M., Lafuente, M. P., Mayor, S., de Imperial, J. M., & Villegas-Pérez, M. P. (2001). Retinal ganglion cell death induced by retinal ischemia neuroprotective effects of two alpha-2 agonists. *Survey of Ophthalmology, 45*(Suppl. 3), S261–S267.

Vidal-Sanz, M., Villegas-Pérez, M. P., Bray, G. M., & Aguayo, A. J. (1993). Use of peripheral nerve grafts to study regeneration after CNS injury. *Neuroprotocols, 3*, 29–33.

Villegas-Pérez, M. P., Lawrence, J. M., Vidal-Sanz, M., Lavail, M. M., & Lund, R. D. (1998). Ganglion cell loss in RCS rat retina: A result of compression of axons by contracting intraretinal vessels linked to the pigment epithelium. *Journal of Comparative Neurology, 392*, 58–77.

Villegas-Pérez, M. P., Vidal-Sanz, M., Bray, G. M., & Aguayo, A. J. (1988). Influences of peripheral nerve grafts on the survival and regrowth of axotomized retinal ganglion cells in adult rats. *Journal of Neuroscience, 8*, 265–280.

Villegas-Pérez, M. P., Vidal-Sanz, M., & Lund, R. D. (1996). Mechanism of retinal ganglion cell loss in inherited retinal dystrophy. *NeuroReport, 7*, 1995–1999.

Villegas-Pérez, M. P., Vidal-Sanz, M., Rasminsky, M., Bray, G. M., & Aguayo, A. J. (1993). Rapid and protracted phases of retinal ganglion cell loss follow axotomy in the optic nerve of adult rats. *Journal of Neurobiology*, 24 23–36.

Wang, S., Villegas-Pérez, M. P., Holmes, T., Lawrence, J. M., Vidal-Sanz, M., Hurtado-Montalban, N., et al. (2003). Evolving neurovascular relationships in the RCS rat with age. *Current Eye Research, 27*, 183–196.

Wang, S., Villegas-Pérez, M. P., Vidal-Sanz, M., & Lund, R. D. (2000). Progressive optic axon dystrophy and vacuslar changes in rd mice. *Investigative Ophthalmology and Visual Science, 41*, 537–545.

Watanabe, M., Sawai, H., & Fukuda, Y. (1991). Axonal regeneration of retinal ganglion cells in the cat geniculocortical pathway. *Brain Research, 560*, 330–333.

Whiteley, S. J., Sauve, Y., Aviles-Trigueros, M., Vidal-Sanz, M., & Lund, R. D. (1998). Extent and duration of recovered pupillary light reflex following retinal ganglion cell axon regeneration through peripheral nerve grafts directed to the pretectum in adult rats. *Experimental Neurology, 154*, 560–572.

WoldeMussie, E., Ruiz, G., Wijono, M., & Wheeler, L. A. (2001). Neuroprotection of retinal ganglion cells by brimonidine in rats with laser-induced chronic ocular hypertension. *Investigative Ophthalmology and Visual Science, 42*, 2849–2855.

Wood, J. N., & Anderton, B. H. (1981). Monoclonal antibodies to mammalian neurofilaments. *Bioscience Reports, 1*, 263–268.

Yoles, E., & Schwartz, M. (1998). Degeneration of spared axons following partial white matter lesion: Implications for optic nerve neuropathies. *Experimental Neurology, 153*, 1–7.